UC San Diego
UC San Diego Previously Published Works

Title

Tumor necrosis factor receptor-1 is selectively sequestered into Schwann cell extracellular vesicles where it functions as a TNFα decoy

Permalink

https://escholarship.org/uc/item/9nn9t913

Journal

Glia, 70(2)

ISSN

0894-1491

Authors

Sadri, Mahrou
Hirosawa, Naoya
Le, Jasmine
et al.

Publication Date

2022-02-01

DOI

10.1002/glia.24098

Copyright Information

Peer reviewed

GLIA

WILEY

RESEARCH ARTICLE

Tumor necrosis factor receptor-1 is selectively sequestered into Schwann cell extracellular vesicles where it functions as a TNFα decoy

Mahrou Sadri[1] | Naoya Hirosawa[1,2] | Jasmine Le[1,3] | Haylie Romero[1,4] | Stefano Martellucci[1] | Hyo Jun Kwon[1] | Donald Pizzo[5] | Seiji Ohtori[2] | Steven L. Gonias[5] | Wendy M. Campana[1,3,4]

[1]Department of Anesthesiology, University of California, San Diego, La Jolla, California, USA

[2]Department of Orthopaedic Surgery and Graduate School in Medicine, Chiba University, Chiba, Japan

[3]Veterans Administration San Diego Healthcare System, San Diego, California, USA

[4]Program in Neuroscience, University of California, San Diego, La Jolla, California, USA

[5]Department of Pathology, University of California, San Diego, California, USA

Correspondence
Wendy M. Campana, Department of Anesthesiology, University of California, San Diego, 9500 Gilman Drive, La Jolla, CA 92093-0629, USA.
Email: wcampana@health.ucsd.edu

Abstract

Schwann cells (SCs) are known to produce extracellular vesicles (EV) that participate in cell–cell communication by transferring cargo to target cells, including mRNAs, microRNAs, and biologically active proteins. Herein, we report a novel mechanism whereby SC EVs may regulate PNS physiology, especially in injury, by controlling the activity of TNFα. SCs actively sequester tumor necrosis factor receptor-1 (TNFR1) into EVs at high density, accounting for about 2% of the total protein in SC EVs (~1000 copies TNFR1/EV). Although TNFR2 was robustly expressed by SCs in culture, TNFR2 was excluded from SC EVs. SC EV TNFR1 bound TNFα, decreasing the concentration of free TNFα available to bind to cells and thus served as a TNFα decoy. SC EV TNFR1 significantly inhibited TNFα-induced p38 MAPK phosphorylation in cultured SCs. When TNFR1 was proteolytically removed from SC EVs using tumor necrosis factor-α converting enzyme (TACE) or neutralized with antibody, the ability of TNFα to activate p38 MAPK in the presence of these EVs was restored. As further evidence of its decoy activity, SC EV TNFR1 modified TNFα activities in vitro including: (1) regulation of expression of other cytokines; (2) effects on SC morphology; and (3) effects on SC viability. SC EVs also modified the effects of TNFα on sciatic nerve morphology and neuropathic pain-related behavior in vivo. By sequestering TNFR1 in EVs, SCs may buffer against the potentially toxic effects of TNFα. SC EVs provide a novel mechanism for the spatial and temporal regulation of neuro-inflammation.

KEYWORDS
extracellular vesicles, neuropathic pain, peripheral nerve injury, Schwann cells, TNF Receptor-1, TNFα

1 | INTRODUCTION

Injury to the peripheral nervous system (PNS) triggers a series of programmed events referred to as Wallerian degeneration (WD). Successful execution of the WD program is necessary to facilitate

optimal peripheral nerve regeneration and avoid chronic pain states (Chen et al., 2007). TNFα is expressed by activated Schwann cells (SCs) early in the course of WD and regulates many WD events, including expression of secondary cytokines by SCs, such as IL-1β, IL-6, and IL-10 (Myers et al., 2006; Schäfers & Sorkin, 2008; Shamash et al., 2002).

TNFα is active as a membrane-associated trimeric proform and as a soluble cytokine by interacting with two receptors, TNF Receptor 1 (TNFR1) and TNFR2 (MacEwan, 2002). TNFR1 is the primary receptor responsible for activating pro-inflammatory responses in many cells (Guma & Firestein, 2012; Sabio & Davis, 2014). Although TNFR2 has a lower affinity for TNFα (MacEwan, 2002; Skoff et al., 1998), this receptor is substantially upregulated in peripheral nerves 24 h after PNS injury (George et al., 2005). TNFR1 and TNFR2 are both implicated in neuropathic pain (Dellarole et al., 2014; Sommer et al., 1998; Vogel et al., 2006; Zhang et al., 2011). A number of therapeutic approaches have been developed to control TNFα activity in PNS injury, including TNFα-neutralizing antibodies (Onda et al., 2003; Schäfers et al., 2001), soluble TNFR1 ectodomain-containing proteins (Schall et al., 1990), and drugs that inhibit TNFR1-initiated cell-signaling (Campana, Li, Shubayev, et al., 2006; Myers et al., 2003; Schäfers et al., 2003). Understanding how TNFα activity is regulated in nerve injury, in the absence of exogenous modulators, remains an important goal.

Extracellular vesicles (EVs) have emerged as important mediators of intercellular communication in both health and disease (Sato & Weaver, 2018). EVs are produced by diverse cells and include exosomes, which form by budding of multivesicular bodies in the endosomal transport pathway, shedding microvesicles, which form by plasma membrane budding, and apoptotic bodies which form during cell death (Raposo & Stoorvogel, 2013; van Niel et al., 2018). Exosomes are heterogenous in size, ranging from 30 to 150 nm in diameter and express specific biomarkers (Théry et al., 2006). Exosomes mediate cell–cell communication, mainly by transferring cargo to target cells including micro-RNAs, mRNAs, and biologically active proteins (Colombo et al., 2014; De Gregorio et al., 2018; Mathivanan et al., 2010; Sato & Weaver, 2018; Vlassov et al., 2012). Several studies have shown that SC EVs regulate sensory neuron physiology by the cargo transfer mechanism (Chen et al., 2019; Ching et al., 2018; Lopez-Verrilli et al., 2013).

Herein, we identify SC-derived EVs as robust regulators of TNFα. We demonstrate that SCs selectively sequester TNFR1 at high density into SC EVs so that the ratio of TNFR1/TNFR2 is dramatically increased in SC EVs compared with the cell of origin. TNFR1 constitutes about 2% of the total protein in SC EVs and actively binds TNFα. SC EVs substantially attenuate the response of SCs to TNFα by decreasing the concentration of free TNFα available to trigger cell-signaling. The identified "decoy activity" of SC EV TNFR1 may be important for regulating TNFα responses in other cells in the injured PNS as well, including sensory neurons and inflammatory cells. Because binding of TNFα to SC EV TNFR1 is reversible, TNFα may be released from EVs as the local concentration of this cytokine decreases, assuring that the decrease in TNFα is not precipitous. Although TNFR1 has been identified in exosome-like EVs in serum and from lung epithelial cells (Hawari et al., 2004), the selective sequestration of TNFR1 into SC EVs is a novel finding. SC EVs emerge as particles capable of regulating the response to PNS injury both spatially and temporally by a mechanism independent of cargo transport.

2 | MATERIALS AND METHODS

2.1 | Rat primary SC cultures

Primary SC cultures were isolated from postnatal (day 1) rat pups and maintained as described previously (Campana, Li, Dragojlovic, et al., 2006). SCs were cultured in complete medium consisting of Dulbecco's Modified Eagle Medium (DMEM) (Gibco, 11885), supplemented with 10% heat inactivated FBS (Gibco, 10-082-147), 100 U/ml penicillin, 100 μg/ml streptomycin, 21 μg/ml bovine pituitary extract (Sigma, P1476) and 4 μM forskolin (Cell Signaling, 3828S) at 37°C in humidified atmosphere with 5% CO_2. To confirm purity of the primary cultures, isolated SCs were immunostained with anti-S100 β (Abcam, ab52642) overnight at 4°C followed by Alexa Fluor 488 anti-rabbit secondary antibody (Thermofisher, A-11034). After adding mounting media with DAPI (Abcam, ab104139), slides were imaged on an Olympus CKX41 microscope using the Infinity Analyze and Capture Software. Controls without primary antibody revealed no non-specific staining. SCs used for all studies were passaged no more than six times.

2.2 | Isolation of rat SC-derived EVs

SCs were cultured in complete medium until 80% ∼ 90% confluent and then washed gently with warm Dulbecco's phosphate-buffered saline (DPBS) (Gibco, 14190144) to remove exogenous and endogenous EVs. The medium was replaced with DMEM containing 10% FBS which was depleted of EVs by ultracentrifugation (UC) at 100,000g for 18 h (Shelke et al., 2014). The medium was supplemented with 100 U/ml penicillin and 100 μg/ml streptomycin. There was no BPE in the SC medium to avoid co-isolation of exogenous EVs and minimize cell proliferation.

SCs were allowed to condition medium for 15 h. EVs in conditioned medium (CM) were isolated by differential UC, as previously described (Théry et al., 2006) and modified by us. Briefly, CM was centrifuged at 2000g for 10 min to remove cellular debris and then at 11,000g for 30 min at 4°C to remove larger EVs. The resulting supernatant was then subjected to UC at 100,000 x g for 18 h at 4°C to pellet EVs. This pellet was washed in cold 20 mM sodium phosphate, 150 mM NaCl, pH 7.4 (PBS), passed through the 0.22 μm filter, re-pelleted at 130,000g for 3 h at 4°C, and re-suspended in PBS. Fresh and recently frozen SC EVs with equivalent characterization and bioactivity were used for each experiment.

2.3 | Nanoparticle tracking analysis

EVs were analyzed by NTA as previously described (Almanza et al., 2018). Briefly, isolated EVs were analyzed using a NanoSight

NS300 instrument equipped with a 405 violet laser (Malvern). Which was calibrated with 100 and 200 nm polystyrene latex microbeads. EV samples were pushed through a fluidics flow chamber at a constant flow rate using a syringe pump at room temperature. Each sample was measured in triplicate. NTA analytical software version 2.3 was used for capturing and analyzing the data according to the manufacturer's protocol.

2.4 | Transmission electron microscopy

Formvar–carbon-coated copper grids (100 mesh, Electron Microscopy Sciences) were placed on 20 μl drops of each EV-containing solution on parafilm sheets. After allowing adsorption of solution components for 10 min, grids were washed three times with 200 μl drops of Milli-Q water and then incubated for 1 min with 2% (weight/volume) uranyl acetate (Ladd Research Industries). The excess solution was removed with Whatman 3MM blotting paper. Grids were left to dry and then examined using a Tecnai G2 Spirit BioTWIN transmission electron microscope (TEM) equipped with an Eagle 4 k HS digital camera (FEI).

2.5 | Immunoblot analysis of SC EVs

An equivalent amount of protein ($2 \sim 5$ μg), as determined by bicinchoninic acid assay (BCA), was subjected to 10% SDS-PAGE and transferred to nitrocellulose membranes. Membranes were blocked with Blotting grade blocker (5% nonfat dry milk) (Bio Rad, 170-6404) in 10 mM Tris–HCl, 150 mM NaCl, pH 7.5, 0.1% Tween 20 (TBS-T) for 1 h at room temperature. Primary antibodies diluted in 5% BSA/TBST were incubated overnight at 4°C. The primary antibodies used included: anti-CD9 (rabbit monoclonal 1:1000; Novus, NBP2-67310), anti-CD81 (rabbit monoclonal 1:2000; Novus, NBP2-67722), anti-TSG101 (rabbit monoclonal 1:500; Abcam, ab30871), anti-Alix (mouse monoclonal 1:1000; Novus, NB100-65678), anti-Flotillin-1 (mouse monoclonal 1:1000; BD Bioscience, 610,821), anti-GM130 (mouse monoclonal 1:1000; BD Bioscience, 610,822), anti-p75[NTR] (rabbit monoclonal 1:1000; Cell Signaling, 8238 s), anti-myelin protein zero (MPZ) (rabbit polyclonal 1:1000, Abcam, ab183868), anti-GFAP (rabbit polyclonal 1:5000, DAKO, GA524), anti-TNFR1 (rat monoclonal 1:1000; R&D Systems, MAB425), and anti-TNFRII (TNFR2 Rabbit Monoclonal Antibody1:1000, Invitrogen, MA5-32618). Membranes were washed with TBS-T and incubated with secondary HRP-conjugated antibodies (1:2000; Cell Signaling Technology, 7074 and Bio-Rad, 170-6516) in TBS-T with nonfat dry milk for 1 h at room temperature followed by enhanced chemiluminescence (ECL; GE Healthcare). Blots were imaged onto film and scanned (Canonscan). Densitometry was performed using Image J software.

2.6 | Dot blot analysis

To measure TNFα-binding, different amounts of SC EVs in 3 μl final volume were dotted onto nitrocellulose membranes and allowed to air dry for 1 h at room temperature. The membranes were then blocked with 5% milk in TBS-T and subsequently incubated with 1 nM of biotinylated TNFα (R&D, BT210-010) in 0.1% BSA and TBS-T overnight at 4°C and then with streptavidin-HRP-conjugated antibody (R&D DY998). Binding was detected by enhanced chemiluminescence (GE Healthcare). In separate studies, membranes with immobilized EVs were blocked with 5% milk in TBS in the absence of 0.1% (vol/vol) Tween-20, to avoid EV permeabilization, for 1 h at room temperature. Subsequently, membranes were incubated with primary antibodies against TNFR1 (rat monoclonal 1:1000; R&D Systems, MAB425) and then with HRP-conjugated secondary antibody in 5% milk with TBS followed by detection and imaging with ECL (GE Healthcare).

2.7 | TNFα cross-linking studies

To covalently stabilize non-covalent complexes, we used the bifunctional cross-linker, bis (sulfosuccinimidyl) suberate (BS³) (Thermo Fisher, 21580) as previously described (Crookston & Gonias, 1994). Rat SC EVs (10 μg) were incubated with TNFα (0.5 nM, R&D Systems, BT210-010) and then with 5 mM BS³ for 10 min at 37°C. TNFα (0.5 nM) was treated with BS³ in the absence of SC EVs as a control. All samples were subjected to 10% SDS-PAGE and transferred to nitrocellulose membranes. The membranes were blocked with 5% nonfat dry milk (Bio-Rad, 170-6404) in 10 mM Tris–HCl, 150 mM NaCl, pH 7.5, 0.1% Tween 20 (TBS-T) for 90 min at room temperature. Blots were probed with primary TNFα-specific antibody (TNFα mouse monoclonal 1:500, Santa Cruz, sc-133192) (1:1000) overnight at 4°C. Subsequently, the membranes were washed with TBS-T and incubated with secondary mouse HRP-conjugated antibodies (1:2000; Cell Signaling Technology, 7076S) in TBS-T for 1 h at room temperature. Signals were detected by ECL (GE Healthcare).

2.8 | Quantification of TNFR1 in SC EVs

Six independent SC EV preparations (1.0 μg) were subjected to SDS-PAGE and immunoblotting with anti-TNFR1. Different concentrations of recombinant human soluble TNFR1 protein (28-kDa; R&D Systems, 636-R1) were run on the same blots to generate a standard curve. The amount of TNFR1 in each of the six EV preparations was determined by comparison to the standard curve. NTA data were used to calculate the absolute number of EVs in 1.0 μg of EV protein. These data were then used to calculate the mean number of copies of TNFR1 per EV.

2.9 | Analysis of TNFα binding to SCs in vitro by immunofluorescence (IF) microscopy

To study biotinylated TNFα-binding to SCs in culture, SCs were plated in PDL-coated 6-well plates at a density of 3.0×10^5 cells/well and

cultured until ~85% confluent. Biotin-labeled recombinant human TNFα (1 nM) (R&D Systems, BT210-010) and SC-derived EVs (0–5 μg/ml) were added to the cultured SCs for 1 h at 22°C. SCs were fixed with fresh 4% paraformaldehyde in PBS for 10 min. Nonspecific binding sites were blocked with 0.5% TNB blocking solution. Incubations with primary goat polyclonal antibody against human TNFα (1:1000; R&D Systems, AF-510-NA) were performed overnight at 4°C. Fixed cells were then incubated in Alexa-Fluor 564-conjugated secondary antibody (Thermo Fisher, A-11012) for 2 h at 22°C. In control studies, primary antibody was omitted. Preparations were mounted on slides using Pro-long Gold (Abcam, ab104139) with DAPI for nuclear labeling. Images were captured using an Olympus FV1000 confocal microscope with an oil-immersion objective (60 × 1.42 NA).

IF microscopy studies were complemented by immunoblotting studies, in which SCs were washed and then extracted with RIPA buffer (PBS with 1% Triton X-100, 0.5% sodium deoxycholate, 0.1% SDS), protease inhibitor mixture (Roche, 11873580001). An equivalent amount of cellular protein was subjected to SDS-PAGE and electro transferred to nitrocellulose membranes. Membranes were blocked for 1 h in nonfat milk. Biotinylated TNFα was detected with streptavidin-HRP (1:100,000) (R&D Systems, DY998).

2.10 | Treatment of SC EVs with TNFα converting enzyme (TACE)

TNFα converting enzyme (TACE) releases TNFR1 from the plasma membrane (Bell et al., 2007; Rowlands et al., 2011). We tested the ability of TACE to release TNFR1 from SC EVs and thus, deplete these EVs of TNFR1. Equal amounts of SC EVs (100 μg) were treated with TACE (20 or 80 nM) (R&D Systems, 2978-AD) or vehicle for 1 h with agitation. Samples were subjected to UC at 130,000g for 2 h at 4°C. Supernatants, containing released proteins, were separated and retained for analysis. EV-containing pellets (TACE-EV) were washed with PBS, subjected to UC at 130,000g for 2 h again, and also retained for analyses.

2.11 | Analysis of p38 MAPK signaling in vitro

SCs were plated in PDL-coated 6-well plates at a density of 3.0×10^5 cells/well and cultured in complete medium until ~85% confluent. Cells were treated with various proteins and reagents, alone, simultaneously or preincubated as noted, including: TNFα (0–1 nM); SC EVs (10 μg); TACE-EVs (10 μg); TNFR1-neutralizing monoclonal antibody (2.5 or 10 μg, R&D Systems, MAB425); a neutralizing antibody to TNFR2 (2, 4 or 8 μg; MA5-29837, Invitrogen); or IgG (10 μg; Sigma Aldrich, 06-255). In some cases, SCs were electroporated using the Rat Neuron Nucleofector Amaxa Kit (Lonza Biosciences) and incubated with siRNA to silence TNFR2 expression (siTNFR2; M-094191-01-0010, Dharmacon). Control cells were transfected with non-targeting control (NTC) siRNA (NTC; D-001810-10-05, Dharmacon). Cells were treated with TNFα. Cell extracts were

prepared in RIPA buffer, and sodium orthovanadate. The protein concentration was determined by BCA. An equivalent amount of cellular protein (10–20 μg) was subjected to SDS-PAGE and immunoblot analysis. Membranes were incubated with primary antibodies that recognize phospho-p38 MAPK (rabbit polyclonal 1:1000, Cell Signaling, 9211 s) and total p38 MAPK (1:10000, Cell Signaling, 9212 s).

2.12 | RT-qPCR

RNA was isolated from SCs 48 h after electroporation using the NucleoSpin RNA kit (Macherey-Nagel) and reverse-transcribed using the iScript cDNA synthesis kit (Bio-Rad). qPCR was performed using TaqMan gene expression products (Thermo Fischer Scientific). Tnfrsf1b and Tnfrsf1a probes were used to measure expression of the mRNAs encoding TNFR2 and TNFR1, respectively, using CFX Connect Real-Time system (Bio-Rad) and normalized to GAPDH as an internal control. The relative change in mRNA expression was calculated using the $2^{\Delta\Delta CT}$ method with GAPDH mRNA as an internal normalizer (4331182, ThermoFisher). All results are presented as the fold-change in mRNA expression relative to controls (transfected with NTC siRNA).

2.13 | SC morphology in vitro

SC morphology was evaluated 1.5 h after treatment with TNFα (0.5 nM), TNFα plus SC EVs (10 μg), or vehicle (0.01% BSA in PBS). SCs were immunostained with anti-S100 β (1:100, Abcam, ab52642) to identify SC cytoplasm, and with mounting medium containing DAPI (Abcam, ab104139) to label nuclei. Stained SCs were imaged at ×20 using an Olympus CKX41 inverted fluorescence microscope with a Lumenera INFINITY5-5 M digital camera. Images were subjected to image analysis using Image J. Nuclear area and cytoplasmic area (total cell area minus nucleus area) were determined in randomly selected cells by an investigator who was blinded to the experimental groups. Nuclear area/cytoplasmic area (N/C ratios) were calculated for a minimum of 30 cells per field, from three different experimental replicates for each treatment.

2.14 | Cytokine array

Cytokine arrays were performed using the Rat Cytokine Array Panel A (R&D Systems, ARY008). Briefly, SCs were cultured in 6-well plates and upon reaching 85% confluence, the growth medium was replaced with DMEM containing 1% exosome-free FBS and 100 U/ml penicillin and 100 μg/ml streptomycin (1%). TNFα (0.5 nM) alone or TNFα (0.5 nM) plus SC-EVs (10 μg) was added to the SC cultures. After 3 h, stimulated cells were lysed using the recommended lysis buffer modified by us (1% IGEPAL, 20 mM Tris–HCl [pH 8.0], 137 mM NaCl, 10% glycerol, 2 mM EDTA, and Protease inhibitor) for 30 min at 4°C followed by centrifugation at 14,000 g for 5 min. Cell extracts were

incubated with nitrocellulose membranes, pre-loaded with antibodies, as recommended by the manufacturer. Membranes were developed using Thermo Scientific™ SuperSignal™ West Femto Maximum Sensitivity Substrate kit (Thermo Scientific, PI34095) on autoradiography films. Densitometry of each dot was performed using ImageJ.

2.15 | Assessment of SC viability

SCs were plated at 10,000 cells/well in 96-well plates. After attaching to the wells, cells were gently washed and cultured in DMEM containing 1.0% EV-depleted FBS with TNFα (0.5 nM) or vehicle in the presence or absence of SC-derived EVs (0.5 or 1 μg) for 18 h. The Cell Death Elisa™ (Roche, 11774425001) was used to measure SC viability by colorimetric analyses (402 nm). SCs cultured in 10% EV-depleted FBS containing media served as normalizing controls. For Trypan blue studies, 6-well plates with 2.0 x 10^5 SCs were cultured overnight. The next day, medium supplemented with 1.0% EV-depleted FBS was added to the cells together with TNFα (0.5 nM) or TNFα + SC EVs (0–500 ng/ml). Cells that excluded Trypan blue were counted.

2.16 | Analysis of TNFα-induced p38 MAPK activation in vivo

Male Sprague–Dawley rats ($\sim$200 g) were purchased from Envigo (Indianapolis, IN). All procedures were performed according to protocols approved by the University of California, San Diego, Committee on Animal Research and conform to the NIH guidelines for animal use. Rats were randomly assigned into four groups: (1) no treatment; (2) injected with vehicle (3 μl PBS + 0.01% BSA); (3) injected with TNFα (1.0 ng TNFα in 3 μl PBS); (4) injected with TNFα + SC EVs (in 3 μl PBS). Before treatment, the rats were housed in pairs with 12 h light/dark cycle and given ad libitium access to food and water. Before surgery, animals were anesthetized with 5% isoflurane (VetOne, 502017). Anesthesia was maintained with 3% isoflurane. The left sciatic nerve was exposed at the mid-thigh level. Solutions were injected using a 30-gauge Hamilton steel needle. The needle was left in place for 10 s and then withdrawn to avoid leakage from the needle track. After 15 min, nerves at the injection site were collected and homogenized in RIPA buffer. Immunoblot analysis to detect phosphorylated p38 MAPK was performed as described above. GAPDH was used as a loading control.

2.17 | Sciatic nerve histology studies

Sciatic nerves were formalin-fixed and paraffin-embedded. For routine H&E staining, tissue sections were deparaffinized. Slides were incubated in hematoxylin (Richard-Allen Scientific), rinsed, incubated in clarifier to eliminate nonspecific staining, rinsed again, and then incubated in bluing buffer. Sections were subsequently incubated in Eosin-Y, dehydrated through alcohol and xylene, and cover-slipped.

Light microscopy was performed using a Leica DFC420 microscope with Leica Imaging Software 2.8.1 (Leica Biosystems).

2.18 | Pain-related behavior: Tactile allodynia studies

Male Sprague Dawley rats ($n = 18$) were randomly assigned into three cohorts, which were: (1) Injected in the sciatic nerve with vehicle (3 μl); (2) injected with TNFα (0.5 ng in 3 μl); and (3) injected with TNFα (0.5 ng) plus SC EVs (1.8 μg) (total volume 3 μl). The rats were baseline-tested with von Frey filaments for 3 days. The paw withdrawal threshold (PWT) was determined by sequentially increasing and decreasing the stimulus strength and analyzing withdrawal data using the Dixon up-down method, as described previously (Chaplan et al., 1994; Lee-Kubli et al., 2016). Solutions were injected into the left sciatic nerve using a 30-gauge Hamilton steel needle. Postinjection testing was conducted on day 3. In all behavior studies, the experimenter was blinded to group identity. All procedures were performed according to protocols approved by the University of California, San Diego, Committee on Animal Research and conform to the NIH guidelines for animal use.

2.19 | Statistical analysis

Statistical analysis was performed using GraphPad Prism 5.0 (GraphPad Software). Results are presented as the mean ± *SEM*. Cell-signaling, TNFα-cross-linking, biotinylation IF, morphology, cell viability, and cytokine array data were analyzed by one-way analysis of variance (ANOVA) or Kruswalis analysis (for nonparametric data) followed by a Tukey's or Dunn's post hoc test (*p < .05; **p < .01, ***p < .001). A Student's t test was used when only two means were compared. Pain-related behavior data were analyzed by a repeated measures ANOVA followed by a Bonferroni post hoc test.

3 | RESULTS

3.1 | Characterization of SC-derived EVs

Rat SCs were established in primary culture with greater than 98% purity, as determined by S100β immunolabeling (Figure S1a), and maintained for 12 h in EV-depleted medium. CM was collected and subjected to differential UC to isolate EVs, as previously described (Sadri et al., 2020; Théry et al., 2006). Trypan blue exclusion demonstrated that SC viability was greater than 96% during the EV harvesting period (Figure S1b).

Harvested EVs were analyzed by nanoparticle tracking (NTA). The SC EVs distributed into a major peak with a mean diameter of 156 ± 2 nm (Figure 1a). Results of three independent NTA studies were used to determine that 1.0 μg of SC EV protein corresponds to 1.3 x 10^8 EVs. Transmission electron microscopy (TEM) was
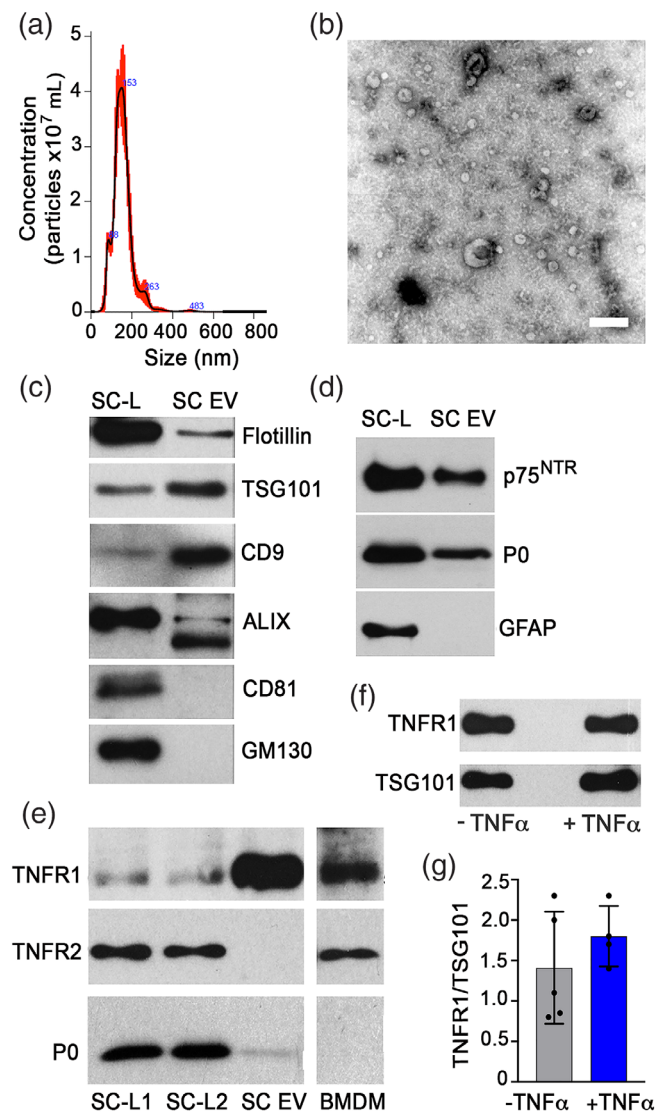
FIGURE 1 TNFR1 is selectively sequestered into SC EVs. (a) SC EVs isolated by UC from conditioned media (CM) of primary cultured SCs were analyzed by NTA and had an average particle size of 153 ± 2 nm; $n = 3$ independent experiments. (b) Transmission electron microscopy (TEM) using negative staining of EVs. Note large crescent shaped particles and smaller particles. Scale bar, 200 nm. (c) Immunoblot analysis of whole SC lysates (SC-L) and SC-derived EVs to detect the exosome biomarkers, Flotillin-1, TSG101, CD9, ALIX, and CD81. GM130 is a Golgi biomarker not found in exosomes. (d) Immunoblot analysis to detect the SC biomarkers, p75^{NTR} and myelin protein zero, P0, and non-myelinating marker, GFAP. Images represent $n = 3$–5 independent experiments. (e) TNFα receptors, TNFR1 (55-kDa) and TNFR2 (65-kDa), and P0 in extracts of SCs cultured in complete medium (SC-L1) or in DMEM with 10% FBS depleted of EVs (SC-L2), in SC-EVs, and in bone marrow derived macrophages (BMDMs) (2 μg/lane) were determined by immunoblot analysis. (f) Immunoblot of TNFR1 levels in EVs derived from SCs treated with and without TNFα. TSG101 (44-kDa) shows load control in cells and presence in EVs. (g) Quantification of TNFR1 levels in SC EV immunoblots (2 μg). Data are expressed as mean ± *SEM*; ($n = 4$-5/group)

performed to examine SC EVs isolated by UC. The EVs were somewhat heterogeneous in size and frequently demonstrated cup-shaped morphology, as anticipated (Figure 1b).

To confirm that SC EVs included exosomes, immunoblot analysis was performed to detect exosome biomarkers. Equal amounts of protein from SC EV extracts and extracts of intact SCs were compared. SC EVs contained the lipid raft-associated protein, flotillin, the cytosolic marker, TSG101, the ESCRT-associated protein, ALIX, the tetraspanin membrane protein CD9, but not CD81 (Figure 1c). GM130, a Golgi apparatus marker that is reported to be excluded from EVs (Lötvall et al., 2014; Merianda et al., 2009) was indeed absent from the SC EV extracts (Figure 1c). These results demonstrate that the SC EV preparations studied here were free of contaminants due to cell debris or cell death.

The SC biomarkers, p75^{NTR} and P0, were detected in extracts of SC EVs (Figure 1d). Although P0 is known to be expressed by cultured SCs, the level of P0 is substantially lower than that observed in intact nerve in which many SCs produce myelin (Brunden & Brown, 1990; Cheng & Mudge, 1996). The non-myelinating SC marker, GFAP, was not detected in SC EVs.

3.2 | SC EVs are highly enriched in TNFR1

Immunoblot analysis was performed to compare TNF receptor protein expression in intact SCs and SC EVs. Extracts of rat bone marrow-derived macrophages (BMDMs) were examined as a control. Both TNFR1 and TNFR2 were detected in cultured SCs (Figure 1e). Compared with BMDMs, the ratio of TNFR2/TNFR1 appeared higher in SCs. When an equivalent amount of protein from SC EVs was probed, the level of TNFR1 was robustly increased, compared with that detected in SCs. TNFR2 was entirely excluded from SC EVs, at the level of detection of the immunoblotting technique. P0 was present in intact SCs and to a lesser extent in SC EVs. P0 was not present in BMDMs, as anticipated. When SC EVs were harvested from SCs that were treated with TNFα or vehicle, the abundance of TNFR1 in the SC EVs was equivalent (Figure 1f,g).

3.3 | SC EVs bind TNFα and compete with SCs for TNFα

Increasing amounts of SC EVs were immobilized on nitrocellulose membranes and probed with TNFR1-specific antibody. TNFR1 was detected and the signal increased as a function of the amount of SC EVs immobilized (Figure 2a). Because these incubations were performed without permeabilizing the EVs, we interpret these results to indicate that the TNFR1 epitope detected by our antibody was externalized in the EV plasma membrane.

To quantify TNFR1 expression in SC EVs, we generated standard curves in which known amounts of purified recombinant soluble TNFR1 ectodomain (28-kDa) were probed by immunoblot analysis (Figure 2b). Band intensity was determined by densitometry. Six separate SC EV preparations were probed on the same immunoblots and the amount of TNFR1 (full-length 55-kDa) was determined by comparison to the standard curve. Applying our analysis of the number of EVs/μg EV protein, determined by NTA, we calculated the number of copies of

TNFR1 per SC EV in each of the six SC EV preparations. Assuming a trimeric structure for TNFR1, as it exists in complexes with TNFα, each SC EV had between 360 and 1075 copies of TNFR1 (Figure 2c).

Next, we performed experiments to determine whether SC EV TNFR1 binds TNFα. We used BS3 to covalently stabilize non-covalent TNFα-TNFR complexes. To validate the method, first we exposed purified TNFα to 5 mM BS3 for increasing periods of time. TNFα is a non-covalent trimer of 17-kDa subunits (Tang et al., 1996), which was detected by SDS-PAGE in the absence of BS3 (Figure 2d). When TNFα was incubated with BS3, the 17-kDa monomers were replaced first by SDS-stable 34-kDa dimers and then by 51-kDa trimers. The TNFα preparation studied in this experiment included bovine serum albumin (BSA) as a stabilizer. No evidence of BSA cross-linking to TNFα was observed, providing an important internal negative control.

Next, purified TNFα was incubated with SC EVs. The samples were treated with BS3 and subjected to SDS-PAGE. A prominent band with a mobility slightly greater than 100-kDa was observed (Figure 2e). This is the anticipated mass for the covalently stabilized complex of TNFα with a single copy of TNFR1. In some studies, faint bands were observed in which TNFα may have been covalently coupled to two copies of TNFR1 (not shown).

As a second approach to demonstrate TNFα-binding to SC EV TNFR1, we immobilized four separate SC EV preparations on

nitrocellulose membranes. The membranes were incubated with biotinylated TNFα (bTNFα) and then with Streptavidin-horseradish peroxidase (S-HRP). As shown in Figure 2f, background binding of S-HRP was detected in all of the SC EV preparations tested in the absence of TNFα; however, a marked increase in signal was observed when SC EVs were pre-treated with bTNFα, indicating TNFα-binding.

To determine whether SC EVs bind TNFα in culture, primary rat SCs were incubated with human TNFα in the presence or absence of SC EVs for 1 h at 22°C and then with Alexa-594-conjugated antibody that specifically detects human TNFα. The IF microscopy images shown in Figure 3a were counterstained with DAPI to show nuclei and obtained at equivalent exposure. Incubation with TNFα substantially increased the TNFα signal observed in association with the SCs. Minimal cross reactivity with rat TNFα was observed in vehicle-treated cells. TNFα-binding to individual cells appeared uniform across different cells, indicating that TNFα receptors are not selectively expressed by a subset of the cells in culture. When SC EVs were included in the incubation, association of TNFα with the cultured SCs was substantially decreased.

Equivalent experiments were performed in which binding of TNFα to SCs was assessed by immunoblot analysis. TNFα was incubated with SCs for 1 h at 22°C. The cultures were washed extensively, and extracts were prepared. Intact 17-kDa TNFα monomer was readily detected in extracts of SCs incubated with TNFα in the absence of
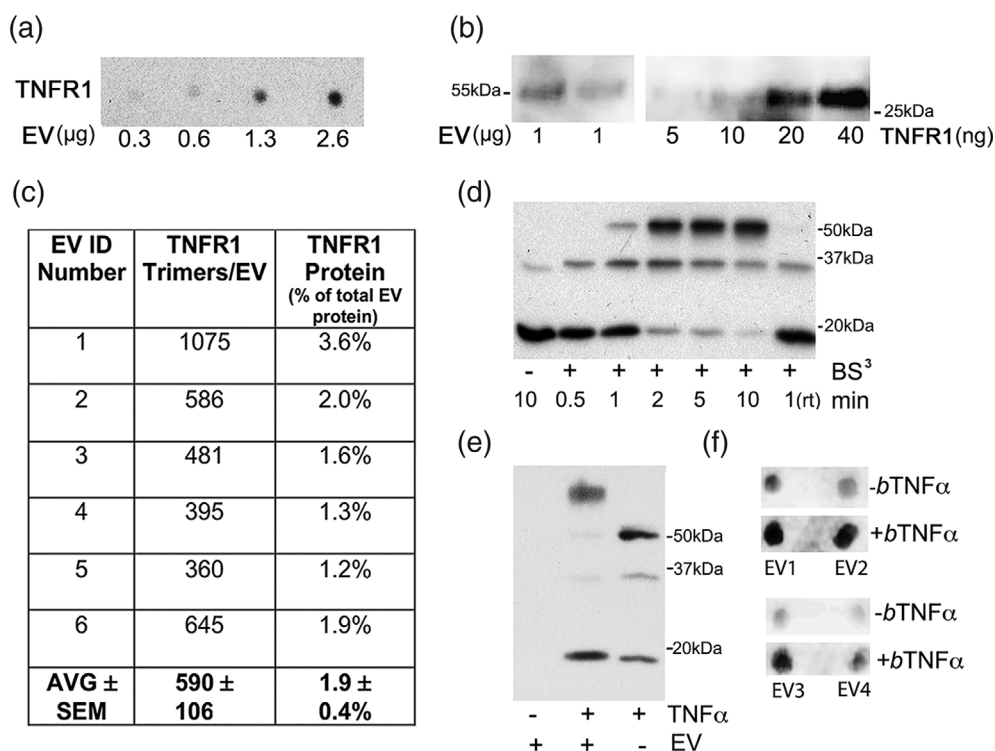

FIGURE 2 TNFR1 is expressed on the surface of SC EVs and binds TNFα in vitro. (a) Representative dot blot of non-permeabilized SC EVs (0–2.5 μg) probed with anti-TNFR1 antibody ($n = 3$ independent blots). (b) Standard curve showing recombinant soluble TNFR1 (28-kDa) and two representative SC EV samples (1 μg/lane). (c) Quantification of the TNFR1 copy number based on the TNFR1 standard curve, NTA and BCA analysis of six independent EV preparations. Data are expressed as the mean ± SEM. (d) Representative immunoblot of TNFα treated with the crosslinker, BS3 (+), or with vehicle (−) for the indicated times at 37°C. (e) Representative immunoblot of SC EVs, SC EV + TNFα and TNFα alone treated with BS3. Note the high molecular mass band in sample of EVs plus TNFα, compared with TNFα alone. (f) Dot blot of four independent SC EV preparations (EV1–4; 1 μg) incubated with or without biotinylated TNFα and probed with S-HRP

SC EVs (Figure 3b). When SC EVs were included in the culture medium (5 μg/ml), TNFα-binding to the cells was inhibited, confirming our IF results. We subjected our immunoblots to densitometry. The results of three different studies are summarized in Figure 3c.

Next, we incubated SCs with TNFα in the presence and absence of EVs and probed the medium for TNFα by immunoblotting. TNFα in the medium included free TNFα and TNFα that was associated with SC EVs. Greatly increased levels of TNFα were detected in the medium when 5 μg/ml of SC EVs were included in the incubation (Figure 3d).

3.4 | SC EVs regulate p38 MAPK activation by TNFα

We examined p38 MAPK phosphorylation in SCs as an index of the response to TNFα. In preliminary studies, we established that the lowest TNFα concentration required to induce p38 MAPK phosphorylation in cultured SCs is 0.5 nM (Figure S2a). Treating SCs with TNFα (0.5 nM) for 8 min increased phospho-p38 MAPK and this increase was blocked by SC EVs (10 μg/ml) (Figure 4a). Exposing SCs to SC EVs (10 μg/ml) in the absence of TNFα caused no significant change in p38 MAPK phosphorylation (Figure S2b). Densitometry results of

10 separate experiments were averaged to demonstrate that the effects of SC EVs on p38 MAPK phosphorylation in TNFα-treated SCs were significant (Figure 4b).

Next, we treated SCs with TNFα in the presence or absence of 2.5 or 10 μg/ml of TNFR1-neutralizing antibody (TNFR1 Ab). The antibody failed to inhibit p38 MAPK phosphorylation in response to TNFα, suggesting that the cellular response of SCs to TNFα is mediated by TNFR2 (Figure 4c). However, when SC EVs were pre-incubated with the same TNFR1 antibody and then added to the cultured SCs together with TNFα, the ability of the SC EVs to block p38 MAPK phosphorylation in response to TNFα was neutralized (Figure 4d).

To confirm that EV-associated TNFR1 is responsible for the TNFα-neutralizing activity of SC EVs, we treated SC EVs with TACE, which releases TNFR1 from plasma membranes in cells (Rowlands et al., 2011; Bell et al., 2007; Hawari et al., 2004). Following TACE treatment, SC EVs were separated from solution components. Figure 4e shows that TNFR1 was removed from the SC EVs by TACE by 20 or 80 nM TACE, and that the TNFR1 was recovered in the supernatant as a product with a molecular mass of ∼43-kDa. The ability of TACE to release TNFR1 from EVs has not been previously reported. Control EVs that were not TACE treated but still subjected to the same washing protocol are shown together with TACE-treated
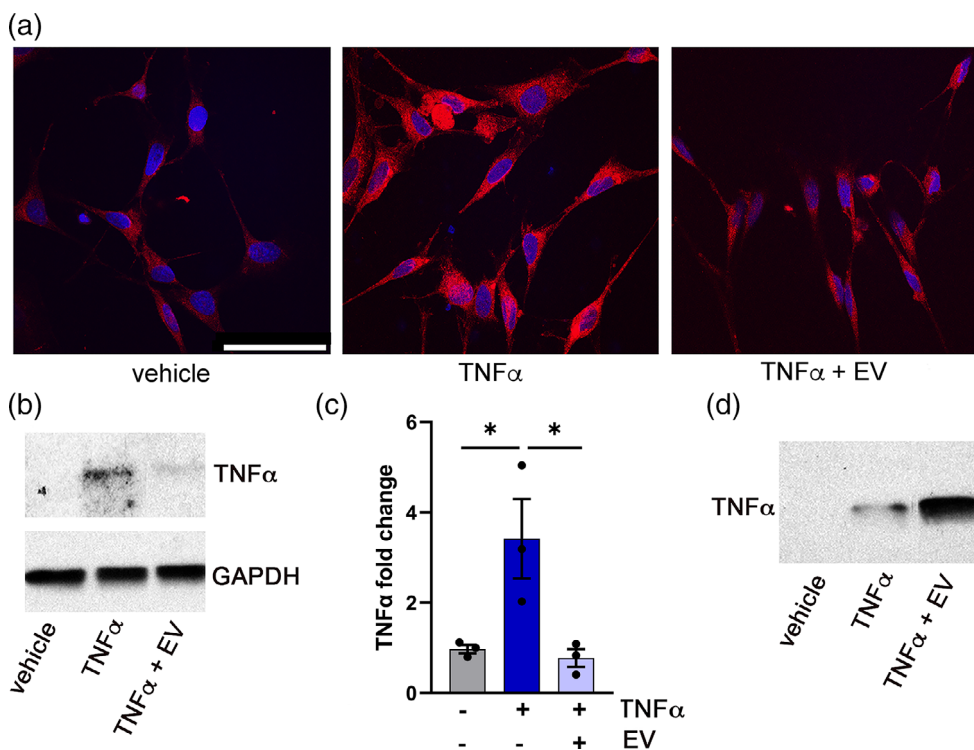

FIGURE 3 SC EV TNFR1 functions as a decoy by binding TNFα and inhibiting its association with cells. (a) Representative IF microscopy images identifying cell associated TNFα (red) and SC nuclei with DAPI (blue) in non-permeabilized SCs. Primary SCs were treated with TNFα (1 nM) in the presence or absence of SC EVs (5 μg) for 1 h and fixed in 4% paraformaldehyde. Scale bar, 50 μm. (b) Immunoblot of TNFα in SC extracts after incubating SCs with TNFα in the presence or absence of SC EVs (5 μg) for 1 h. Membranes were re-probed with GAPDH as a loading control (lower panel). (c) Densitometry analysis showing SC EV-induced reductions in cell-associated TNFα, standardized to the loading control (mean ± SEM; n = 3/group; *p < .05 using a one-way ANOVA and a Tukey's post hoc test). (d) Immunoblot analysis identifying TNFα (1 nM) in SC CM after incubating SCs with TNFα in the presence or absence of SC EV (5 μg) for 1 h
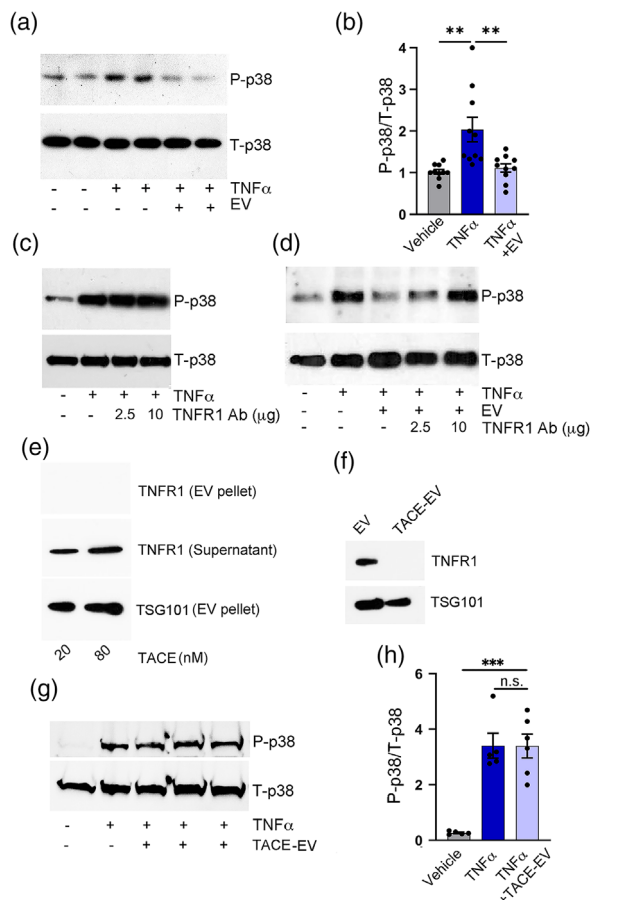
FIGURE 4 SC EVs attenuate TNFα-induced p38 MAPK activation in vitro. (a) Representative immunoblot showing activation of p38 MAPK (P-p38) by TNFα (0.5 nM) and the effects of SC EVs (10 μg), when added simultaneously. Membranes were re-probed for total p38 MAPK (T-p38) as a loading control. Equal amounts of protein extracts (20 μg) were loaded into each lane. (b) Densitometry analysis was performed to determine the relative level of P-p38 standardized against T-p38 (mean ± SEM; $n = 10$ independent experiments, **$p < .01$, vehicle versus TNFα; **$p < .01$, TNFα versus SC EV using a one-way ANOVA with a Tukey's post hoc test). (c) Representative immunoblot showing that TNFα (0.5 nM) activates p38 MAPK and that activation is not blocked by two concentrations of pre-incubated TNFR1-neutralizing antibody. (d) Immunoblot analysis of phospho-p38 MAPK in response to TNFα in the presence or absence of SC EVs. SC EVs were added to cultures together with TNFR1 neutralizing antibody (TNFR1 Ab; 2.5 or 10 μg) as indicated. The blot is representative of three independent experiments. (e) Immunoblot analysis of TNFR1 in pellet and supernatant of SC EVs treated with TACE/ADAM17 (20 or 80 nM). TSG101, an EV biomarker is identified in the pellet. Equal amounts of protein extracts (12 μg) were loaded into each lane. (f) Immunoblot analysis of TNFR1 in control SC EVs and TACE-treated SC EVs. TSG101 serves as a loading control. (g) Representative immunoblot showing activation of p38 MAPK by TNFα (0.5 nM) and the effects of independent preparations of TACE-EVs (10 μg/ml). Membranes were re-probed for T-p38 as a loading control. Equal amounts of protein extracts (20 μg) were loaded into each lane. (h) Densitometry analysis was performed to determine the relative level of P-p38 standardized against T-p38 (mean ± SEM; $n = 6$ independent experiments, ***$p < .001$, vehicle versus TNFα; ***$p < .001$ vehicle versus TNFα + TACE-EV; $p = .997$, n.s. TNFα versus TACE-EV using a one-way ANOVA with a Tukey's post hoc test)

EVs in Figure 4f. TNFR1 is present in the control SC EVs, as anticipated, but not in TACE-EVs. The preparations were probed with TSG101, to confirm recovery of the EVs.

Next, we preincubated TACE-EVs with TNFα and then added these EVs to cultured SCs, replicating the protocol applied in Figure 4a,b. In the absence of TACE-EVs, TNFα (0.5 nM) increased phospho-p38 MAPK and importantly, the increase in phospho-p38-MAPK was not blocked by the TACE-EVs (10 μg/ml) (Figure 4g). Densitometry analysis of six replicates is reported in Figure 4h, confirming that SC EVs do not inhibit TNFα when the TNFR1 is proteolytically removed with TACE.

To determine whether p38 MAPK activation by TNFα in cultured SCs is mediated by TNFR2, we silenced TNFR2 expression with siRNA (siTNFR2) and performed studies with a neutralizing TNFR2 antibody. SCs transfected with siTNFR2 showed significantly decreased expression of TNFR2 mRNA compared with cells transfected with NTC siRNA for 48 h (Figure 5a). TNFR2 protein also was significantly reduced after 48 h (Figure S3). When SCs transfected with NTC siRNA were treated with TNFα, p38 MAPK was activated, as anticipated. By contrast, p38 MAPK was not activated by TNFα in cells transfected with TNFR2-specific siRNA (Figure 5b). As a control, we determined TNFR1 mRNA levels in cells transfected with TNFR2-specific siRNA are unchanged, Thus, siTNFR2 siRNA is specific (Figure 5c).

Next, we pre-incubated cultured SCs with a neutralizing antibody to TNFR2 or IgG control. TNFα activated p38 MAPK in cells treated with IgG alone: However, TNFR2 antibody dose-dependently reduced phospho-p38 MAPK in response to TNFα (Figure 5d). Collectively, these results support the conclusion that activation of p38 MAPK by TNFα in SCs is mediated by TNFR2.

3.5 | SC EVs regulate the effects of TNFα on SC morphology and viability in vitro

Immunofluorescence microscopy of SCs treated with TNFα (0.5 nM) for 1.5 h and stained with the cytoplasmic marker, S100β, showed narrow cell bodies with long process extrusions. This morphology is consistent with the known effects of TNFα on the SC cytoskeleton (Silveira et al., 2018). When SCs were treated with TNFα together with SC EVs, changes in cellular morphology were prevented. Instead, the cells appeared more flattened and spread out on the substratum, as anticipated (Weiner et al., 2001), and similar to control cells that were not treated with TNFα (Figure 6a).

Densitometric analysis of SCs (90 cells/group) treated with vehicle, TNFα, or TNFα + SC EVs revealed a significant increase in the nucleus to cytoplasm (N/C) ratio following TNFα treatment. When SCs were treated with both TNFα and SC EVs, the N/C ratio remained similar to that observed in vehicle-treated control cells (Figure 6b).

To compare cytokine levels in TNFα-treated SCs, in the presence and absence of SC EVs, we performed an unbiased chemokine/cytokine array analysis profiling 29 distinct chemokines and cytokines. SCs were treated with TNFα alone or with TNFα + SC EVs for 3 h. Because the culture medium was supplemented with EV-depleted
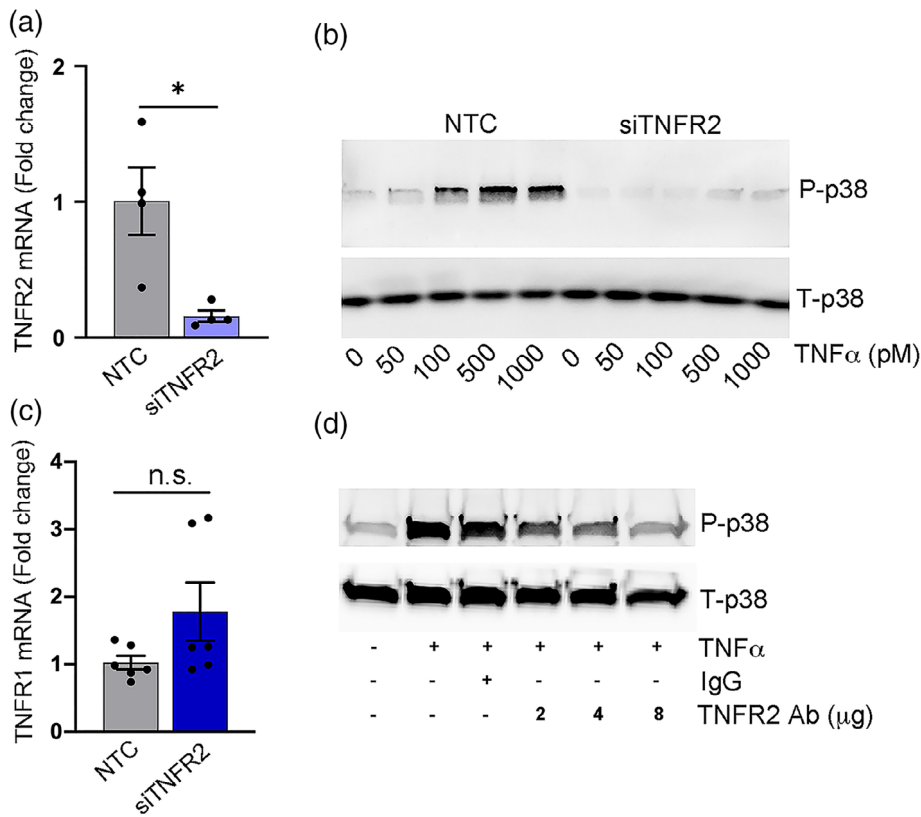
FIGURE 5 TNFR2 mediates TNFα induced P38 MAPK pathway in cultured SCs. (a) RT-qPCR analysis of TNFR2 mRNA after transfection with TNFR2 siRNA for 48 h. Data are presented as mean ± *SEM*; $n = 4$ independent experiments, *$p < .05$ using a *t* test. (b) Representative immunoblot analysis of phospho-p-38 MAPK (P-p38) that is dose-dependently increased by TNFα (8 min) in NTC cells, but not in cells transfected with TNFR2-specific siRNA ($n = 3$). (c) RT-qPCR analysis of TNFR1 mRNA after TNFR2 siRNA transfection for 48 h. Data are presented as mean ± *SEM*; $n = 6$ independent experiments, n.s. using a *t* test. (d) Representative immunoblot analysis of P-p38 after TNFα (0.5 nM) stimulation for 8 min in SCs treated dose-dependently with neutralizing anti-TNFR2 antibody (0–8 µg) or IgG control (8 µg)
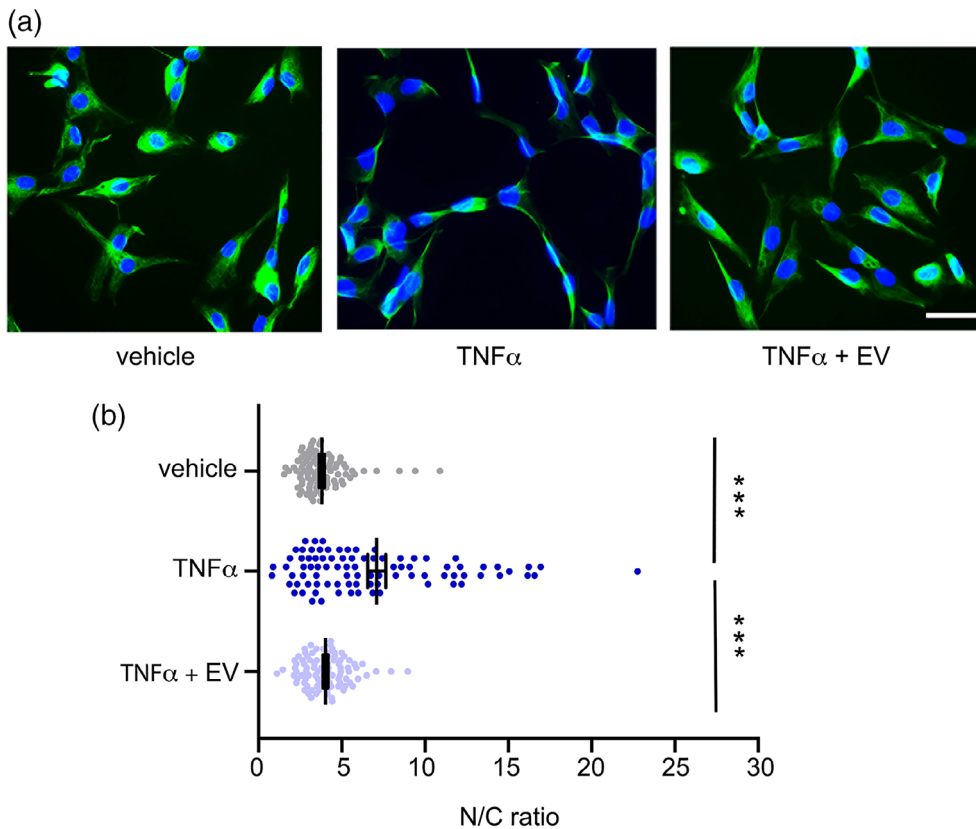

FIGURE 6 SC EVs promote cell morphology changes in SCs following TNFα exposure. (a) Immunofluorescence of S100β in primary cultured SCs treated with vehicle, TNFα (0.5 nM), or TNFα + SC EVs (10 µg) for 1.5 h. Dapi (blue) labels nuclei. Scale bar, 30 µm. (b) Quantitative analysis of S100β immunofluorescence and Dapi. The N/C ratio of SCs treated with TNFα or TNFα in the presence of SC EVs was calculated (mean ± *SEM*.; $n = 30$–40 cells across three biological replicates, ***$p < 0.001$, one-way ANOVA and Tukey's post hoc test)
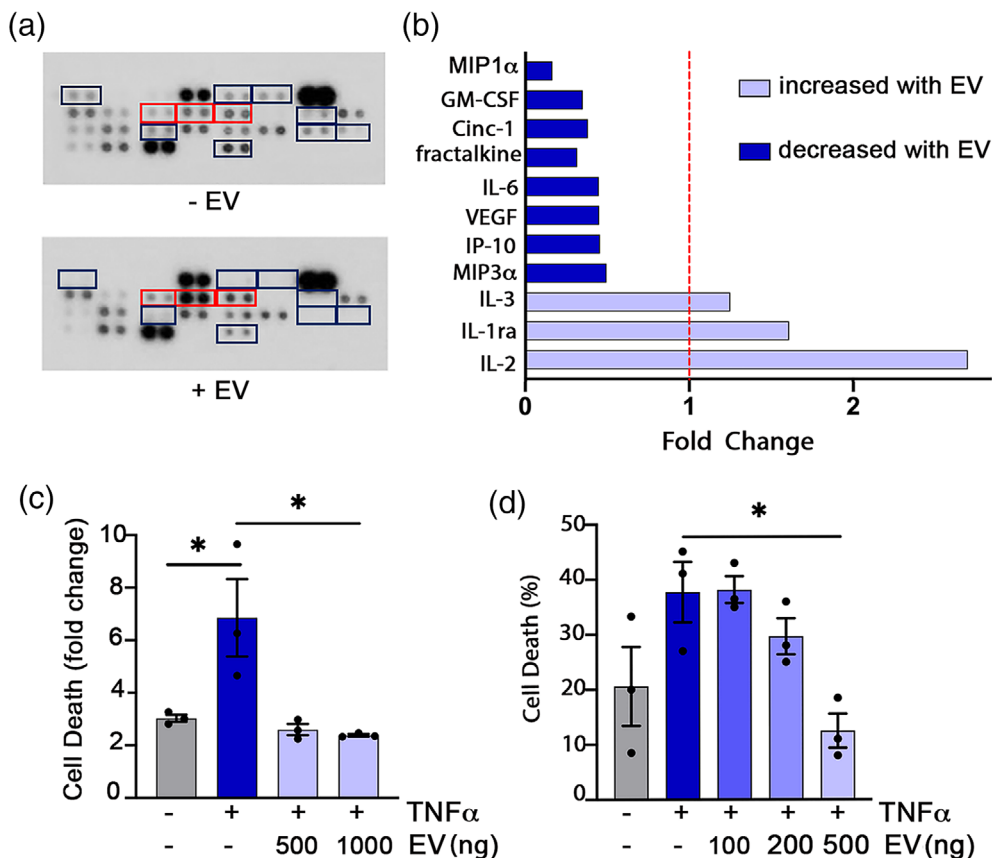
FIGURE 7 Effect of SC EVs on TNFα-mediated cytokine production and cell death. (a) Array analyses of cytokines in SC cell lysates after incubating SCs with TNFα or TNFα plus SC EVs for 3 h. Duplicate dots representing individual cytokines that were increased in abundance by greater than 1.3-fold by EVs, or decreased by greater than 50% by EVs, are indicated by colored boxes. (b) Densitometric analysis of cytokines regulated by SC EVs in SCs treated with TNFα. Data are expressed as the fold-change in cells treated with TNFα + SC EVs versus TNFα alone. (c) Cell death Elisa™ results are shown. TNFα (0.5 nM) treatment for 18 h increased SC death by sevenfold compared with control conditions (10% EV-depleted FBS containing media) and > twofold compared with vehicle control (1% EV-depleted FBS containing media). The increase in cell death was attenuated by co-treatment with SC EVs (0.5 or 1.0 μg) (mean ± *SEM*; $n = 3$ independent experiments, *$p < .05$ using a one-way ANOVA with a Tukey's post hoc test). (d) Dose-dependent effects of SC EVs on SCs treated with TNFα was determined by trypan blue exclusion assay (mean ± *SEM*; $n = 3$ independent experiments, *$p < .05$ using a one-way ANOVA with a Tukey's post hoc test)

FBS, we chose to analyze cell extracts. Changes in cytokine protein expression in SCs treated with TNFα for 3 h have been shown previously (Mazumder et al., 2010; Plaisance et al., 2008). Eleven cytokines and chemokines were either increased in abundance by >30% or decreased >50% when SC EVs were present (Figure 7a). Factors that were downregulated by SC EVs including MIP1α, GM-CSF, Cinc-1, fracktalkine, IL-6, VEGF, IP-10, and MIP3α, which are previously reported to be regulated in PNS injury (Be' eri et al., 1998; Bhangoo et al., 2007; Elliott et al., 2009; Perrin et al., 2005; Rotshenker, 2011; Sondell et al., 1999; Zhang et al., 2013). SC EVs increased levels of the anti-inflammatory factor, IL-1ra (Figure 7b). Interleukin-2, a cytokine known to act as both a pro-inflammatory and anti-inflammatory factor with analgesic properties in the PNS (Nelson, 2004), was substantially increased.

The Cell Death Elisa™, which detects intracytoplasmic oligonucleosomes, was used to measure TNFα-induced SC death, as previously described (Boyle et al., 2005; Mantuano et al., 2011). SCs were cultured in 1% EV-depleted FBS-containing medium with TNFα (0.5 nM), vehicle,

or TNFα + SC EVs. SCs cultured in 10% EV-depleted FBS-containing medium served as the control condition. SCs treated with TNFα demonstrated a sevenfold increase in cell death compared with cells maintained in 10% FBS and about a twofold increase in cell death compared with cells transferred to 1% FBS (Figure 7c). When SC EVs (0.5 or 1 μg) were added together with TNFα, cell death was significantly decreased and similar to that observed when cells were treated with vehicle alone. In trypan blue exclusion experiments, 38% of the SCs treated with TNFα for 24 h were nonviable. SC EVs dose-dependently reduced cell death to ~15% (Figure 7d). Taken together, these results suggest that SC EVs attenuate the effects of TNFα on SC physiology.

3.6 | Demonstration of SC EV TNFα decoy activity in vivo

To examine the effects of SC EVs on TNFα in vivo, we injected TNFα or vehicle into the sciatic nerves in rats. Injection of TNFα increased

phospho-p38 MAPK in nerves compared with nerves that were injected with vehicle. When TNFα was injected together with SC EVs, phospho-p38 MAPK was decreased (Figure 8a). Densitometric analyses of four separate experiments are summarized in Figure 8b. Phospho-p38 MAPK in TNFα-injected nerves was significantly different from that observed in control nerves or nerves injected with TNFα plus SC EVs.
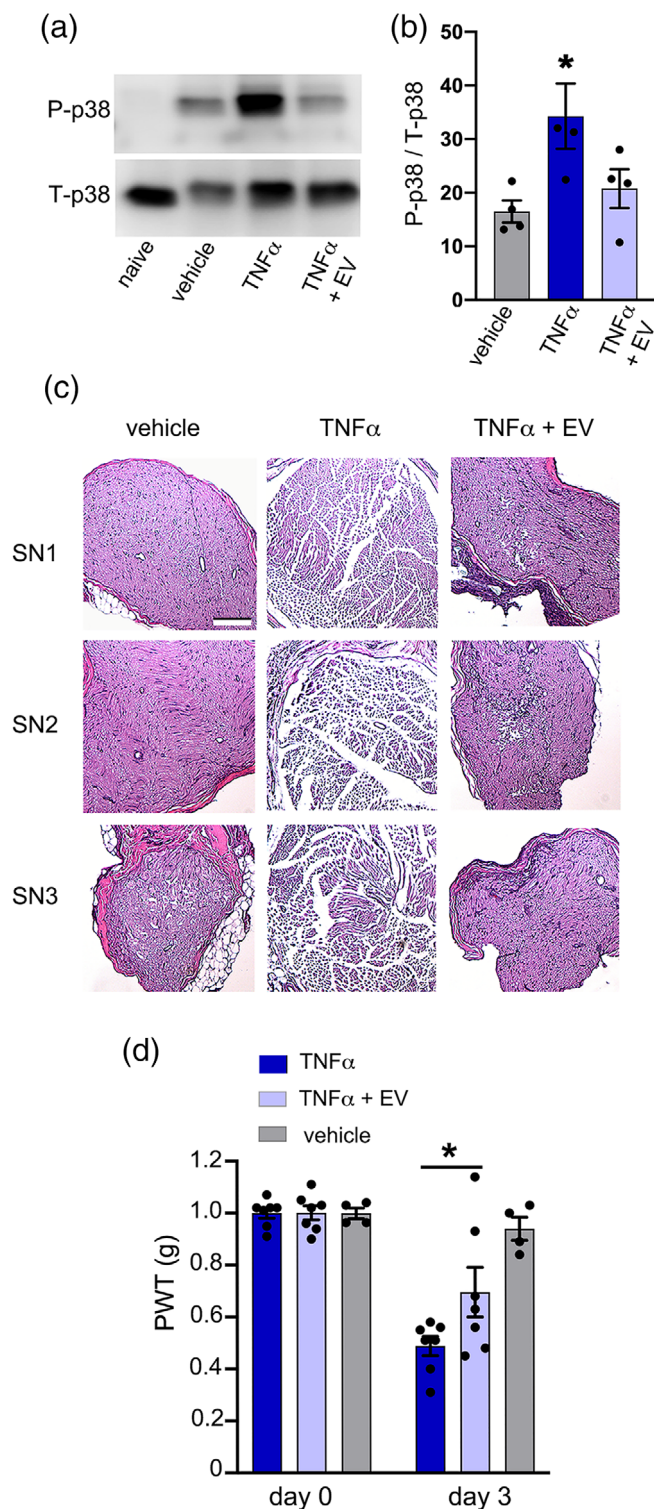
Next, we injected rat sciatic nerves with TNFα, TNFα and SC EVs, or vehicle. Nerves were harvested 3 days after injection and stained with hematoxylin and eosin for histologic examination. Injection of TNFα, in three separate animals, induced edema, which manifested as separation of axons (Figure 8c). These effects of TNFα are consistent with those reported previously (Wagner et al., 1998; Wagner & Myers, 1996). When sciatic nerves were injected simultaneously with TNFα and SC EVs, the effects of TNFα on nerve morphology were attenuated. Nerves isolated from rats injected with TNFα plus SC EVs or vehicle were indistinguishable to an investigator blinded to treatment groups.

3.7 | SC EVs reduce TNFα-induced tactile allodynia in rats

Tactile allodynia is transiently observed in rats following injection of TNFα into the sciatic nerve and is maximal after 3 days (Sorkin & Doom, 2000; Wagner & Myers, 1996). To measure tactile allodynia, we applied von Frey hairs. Baseline testing was conducted for 3 days prior to intraneural injection of TNFα. PWTs were 18.0 ± 1.0 g on day −2, 11.9 ± 0.5 on day −1, and 14.8 ± 0.2 on day 0. Rats were randomized into three groups receiving the following injections: 1) vehicle control; 2) TNFα (0.5 ng); and 3) TNFα (0.5 ng) + SC EVs (2 μg) which were delivered in an equivalent 3 μl volume in each group.

Consistent with previous reports (Wagner et al., 1998; Wagner & Myers, 1996), tactile allodynia was significantly increased by TNFα, 3 days after injection, as indicated by a decrease in PWT compared to day 0 baseline measurements. When TNFα was coadministered with SC EVs, the effects of TNFα on PWTs were significantly attenuated (Figure 8d). Injection of vehicle induced no change in PWTs compared with baseline.

FIGURE 8 SC EVs block the effects of TNFα on sciatic nerve morphology and pain in vivo. (a) Representative immunoblot showing activation of p38 MAPK in naïve sciatic nerve (no injury), in sciatic nerve 15 min after injection of vehicle, TNFα (1 ng), or TNFα (1 ng) plus SC EVs (0.5 μg). (b) Densitometry analysis was performed to determine the relative levels of P-p38 MAPK standardized to the loading control (mean ± SEM; $n = 4$/group; *$p < .05$ compared with control group by a Kruskal-Wallis test and a Dunn's multiple comparisons test). (c) Sciatic nerves were injected with TNFα (0.5 ng), TNFα plus SC EVs (1.8 μg), or vehicle as indicated. Images of individual (SN1, SN2, SN3) rat sciatic nerves (H&E-stained transverse sections) harvested immediately distal to the injection site after 3 days. Note edema induced by TNFα alone is not observed in the two other groups (magnification ×100; scale bar 100 μm). (d) Rats were baseline tested with von Frey hairs for 3 days prior to a one-time injection with vehicle (0.01% BSA), TNFα (0.5 ng), or TNFα + SC EV (1.8 μg). PWTs were determined on day 3 (mean ± SEM; $n = 4$–7/group; *$p < .05$ as compared with the corresponding basal PWTs and between TNFα and TNFα + SC EV using a repeated measures ANOVA with a Bonferroni post hoc test)

4 | DISCUSSION

In response to PNS injury, SCs serve as "first responders," undergoing rapid and substantial phenotypic changes during WD that are essential for functional nerve recovery. SCs are highly integrated in innate immunity; they produce and respond to TNFα early in WD (Myers et al., 2006), establish chemotaxis signals for recruitment of inflammatory cells (Schäfers & Sorkin, 2008), and demonstrate phagocytic activity (Gomez-Sanchez et al., 2015). Regulation of TNFα activity by SCs after injury is thus critical and must occur both spatially and temporally, as the injured nerve transitions from a state in which inflammation and clearance of damaged debris are essential to one in which healing and functional regeneration are paramount. This study demonstrates a novel pathway by which SCs may regulate TNFα activity in the injured nerve microenvironment. We show that SCs generate EVs that are highly enriched in TNFR1. The TNFR1 is functional as it binds TNFα and competes with cellular receptors in SCs for binding of TNFα. SC-derived EVs attenuate the activity of TNFα in vivo in sciatic nerves. As a result, SC EVs regulate: (1) TNFα-induced cell-signaling in the sciatic nerve; (2) TNFα-induced changes in nerve structure; and (3) TNFα-induced tactile allodynia. Similarly, in cell culture, SC-derived EVs block TNFα-induced p38 MAPK activation, TNFα-induced SC morphology changes, changes in cytokine expression, and the effects of TNFα on SC survival. These results indicate that SC EVs function as decoys to regulate TNFα activity. The effects of SC EVs of SC signaling were neutralized when TNFR1 was deleted from the EVs with TACE or incubated with anti-TNFR1. Thus, TNFR1-enriched SC EVs may provide a robust pathway by which EVs limit the activity of TNFα in the injured PNS.

A number of pathways that regulate the activity of TNFα have already been described (Levine, 2004). Examples include: (1) generation of soluble TNFα receptors (Aderka et al., 1992; Levine, 2004); (2) extracellular proteins such as α2-macroglobulin, which bind and neutralize TNFα (Wollenberg et al., 1991); and (3) expression of intracellular proteins such as silencer of death domains (SODD) that bind to TNFR1 and limit signaling (Jiang et al., 1999). Compared with these previously described pathways, SC EVs are unique in their capacity to either inhibit or sustain TNFα activity. The complex formed by TNFα with TNFR1 is non-covalent and we hypothesize that when this complex forms on the EV surface, it is not internalized. Thus, when the concentration of free TNFα is high, SC EVs may adsorb a fraction of the free TNFα, decreasing the amount of cytokine available to interact with cellular receptors. As cellular expression of TNFα decreases and the amount of free TNFα decreases, SC EV TNFR1-TNFα complex may dissociate, buffering against a precipitous decrease in the cytokine level.

An extremely important observation is the substantial shift in the ratio of TNFR1/TNFR2 in SC EVs versus intact SCs in culture. This result suggests that sequestration of TNFR1 into exosomes is an active process with the dual function of empowering EVs for TNFα-binding while discharging TNFR1 from the cell. Indeed, TNFR2 in SCs emerges as the main TNFα receptor initiating p38 MAPK cell-signaling in response to TNFα. Expression of TNFR1 in EVs is not limited to SC

EVs; TNFR1 also has been detected in EVs isolated from endothelial cells (Hawari et al., 2004). However, the enrichment of TNFR1, relative to TNFR2, is a novel observation. Understanding whether SCs are unique in their capacity to selectively sequester TNFR1 into EVs, compared with TNFR2, or whether a similar process is operational in other cell types is an important future goal. Because TNFα undergoes endocytosis in association with TNFR1 (Schneider-Brachert et al., 2004), we tested whether TNFα shuttles TNFR1 into multivesicular bodies where exosomes are formed. However, we saw no significant difference in TNFR1 levels in SC EVs when TNFα was present or omitted from the culture medium during the EV harvesting procedure. We therefore conclude that TNFR1 enrichment in EVs occurs in cultured SCs independently of exogenously added TNFα.

Numerous mechanisms have been proposed by which exosomes and other EVs may regulate cell physiology (Sato & Weaver, 2018). Many of these involve their unique ability to transfer molecular cargo between donor cells and recipient cells. Our "decoy" model of SC EV function is less well characterized. Although we focused on how this model may be operational in an autocrine pathway in which SC-derived EVs regulate SC physiology, paracrine regulation of TNFα activity in the injured PNS is certainly possible, especially three to 5 days after nerve injury in rats, when inflammatory cells such as macrophages populate the nerve injury site (Myers et al., 2006). TNFR1 in SC EVs is poised to regulate innate immunity in the injured nerve milieu. While immune responses to injury are essential, if unchecked, a runaway inflammatory response can cause significant nerve and tissue damage resulting in neuropathic pain. From the functional standpoint, SC EVs emerge as similar to engineered nanovesicles that express TNFR1, produced in human HEK293 cells as a novel biologic and candidate therapeutic reagent for controlling TNFα (Duong et al., 2019). Like these nanovesicles, SC EVs have applicability in therapeutics designed for neuropathic pain and perhaps are superior given their natural endogenous characteristics.

The previously demonstrated ability of TNFα, when injected into peripheral nerves, to mimic nerve injury emphasizes the importance of this cytokine as an orchestrator of WD and the response to PNS injury (Wagner et al., 1998; Wagner & Myers, 1996). TNFα regulates subsequent expression of IL-1β, IL-6, and MIP1α in a secondary wave (Bolin et al., 1995; Kiguchi et al., 2010; Myers et al., 2006; Subang & Richardson, 1999; Üçeyler & Sommer, 2008). The activity of SC EVs, demonstrated after injecting EVs into TNFα-treated nerves, provides evidence that these particles may have efficacy in preventing chronic responses to nerve injury.

Exosomes produced by glia other than SCs, including astrocytes and oligodendrocytes (Frühbeis et al., 2012; Krämer-Albers et al., 2007), have been shown to play a significant role in neurodevelopment, neurodegeneration, and neuroprotection (Kalani et al., 2014; Lai & Breakefield, 2012). The reported mechanism underlying these EV activities involves mainly transfer of mRNA and microRNA-containing cargo. miRNAs delivered in astrocyte EVs to neurons regulate transport of proteins that control synaptic stability and neuronal excitability (Chaudhuri et al., 2018). Previously identified

SC exosome cargo includes the mRNAs for GAP43, Tau, Rac1 and RhoA and the microRNAs, miR-18a and miR-182 (Ching et al., 2018). These molecular products may transfer to axons in the PNS and regulate axonal regeneration (Jia et al., 2018; Lopez-Verrilli, 2012). The activity of SC EVs as autocrine regulators of SC physiology and neuro-inflammation has received less attention. In light of the published studies regarding SC EV cargo transfer and our results, SC EVs emerge as multi-functional regulators of physiology and pathological changes, with considerable potential to control temporal and spatial changes in WD and ultimately, neuropathic pain.

CONFLICT OF INTERESTS

The authors claim no competing interests.

AUTHOR CONTRIBUTIONS

Naoya Hirosawa, Mahrou Sadri, Steven L. Gonias, and Wendy M. Campana conceived of and designed the overall study. Mahrou Sadri, Naoya Hirosawa, Jasmine Le, Haylie Romero, Stefano Martellucci, HyoJun Kwon, and Donald Pizzo performed research. Mahrou Sadri, Naoya Hirosawa, Jasmine Le, Stefano Martellucci, Steven L. Gonias, and Wendy M. Campana analyzed data. Naoya Hirosawa and Wendy M. Campana wrote the initial draft of the manuscript. Mahrou Sadri, Steven L. Gonias, and Wendy M. Campana revised the manuscript. Mahrou Sadri, Jasmine Le, Haylie Romero, Stefano Martellucci, Steven L. Gonias, and Wendy M. Campana edited the manuscript. All authors reviewed the final manuscript.

DATA AVAILABILITY STATEMENT

Materials generated under the project will be disseminated in accordance with University/Participating institutional and NIH policies. Depending on such policies, materials may be transferred to others under the terms of a material transfer agreement. Access to databases and associated software tools generated under the project will be available for educational, research and non-profit purposes. Such access will be provided using web-based applications, as appropriate. Publication of data shall occur during the project, if appropriate, or at the end of the project, consistent with normal scientific practices. Research data which documents, supports and validates research findings will be made available after the main findings from the final research data set have been accepted for publication.

ORCID

Jasmine Le https://orcid.org/0000-0002-8521-765X
Stefano Martellucci https://orcid.org/0000-0002-3952-3162
Wendy M. Campana https://orcid.org/0000-0002-9039-1396

REFERENCES

Aderka, D., Engelmann, H., Maor, Y., Brakebusch, C., & Wallach, D. (1992). Stabilization of the bioactivity of tumor necrosis factor by its soluble receptors. *Journal of Experimental Medicine*, 175(2), 323–329. https://doi.org/10.1084/jem.175.2.323

Almanza, G., Rodvold, J. J., Tsui, B., Jepsen, K., Carter, H., & Zanetti, M. (2018). Extracellular vesicles produced in B cells deliver tumor suppressor miR-335 to breast cancer cells disrupting oncogenic programming *in vitro* and *in vivo*. *Scientific Reports*, 8(1), 1–10. https://doi.org/10.1038/s41598-018-35968-2

Be' eri, H., Reichert, F., Saada, A., & Rotshenker, S. (1998). The cytokine network of Wallerian degeneration: IL-10 and GM-CSF. *European Journal of Neuroscience*, 10, 2707–2713. https://doi.org/10.1046/j.1460-9568.1998.00277.x

Bell, J. H., Herrera, A. H., Li, Y., & Walcheck, B. (2007). Role of ADAM17 in the ectodomain shedding of TNFα and its receptors by neutrophils and macrophages. *Journal of Leukocyte Biology*, 82, 173–176. https://doi.org/10.1189/jlb.0307193

Bhangoo, S., Ren, D., Miller, R. J., Henry, K. J., Lineswala, J., Hamdouchi, C., Li, B., Monahan, P. E., Chan, D. M., & Ripsch, M. S. (2007). Delayed functional expression of neuronal chemokine receptors following focal nerve demyelination in the rat: A mechanism for the development of chronic sensitization of peripheral nociceptors. *Molecular Pain*, 3, 1744-8069-3-38. https://doi.org/10.1186/1744-8069-3-38

Bolin, L. M., Verity, A. N., Silver, J. E., Shooter, E. M., & Abrams, J. S. (1995). Interleukin-6 production by Schwann cells and induction in sciatic nerve injury. *Journal of Neurochemistry*, 64(2), 850–858. https://doi.org/10.1046/j.1471-4159.1995.64020850.x

Boyle, K., Azari, M. F., Cheema, S. S., & Petratos, S. (2005). TNFα mediates Schwann cell death by upregulating p75NTR expression without sustained activation of NFκB. *Neurobiology of Disease*, 20(2), 412–427. https://doi.org/10.1016/j.nbd.2005.03.022

Brunden, K., & Brown, D. (1990). Po mRNA expression in cultures of Schwann cells and neurons that lack basal lamina and myelin. *Journal of Neuroscience Research*, 27(2), 159–168. https://doi.org/10.1002/jnr.490270206

Campana, W. M., Li, X., Dragojlovic, N., Janes, J., Gaultier, A., & Gonias, S. L. (2006). The low-density lipoprotein receptor-related protein is a pro-survival receptor in Schwann cells: Possible implications in peripheral nerve injury. *Journal of Neuroscience*, 26(43), 11197–11207. https://doi.org/10.1523/JNEUROSCI.2709-06.2006

Campana, W. M., Li, X., Shubayev, V. I., Angert, M., Cai, K., & Myers, R. R. (2006). Erythropoietin reduces Schwann cell TNF-α, Wallerian degeneration and pain-related behaviors after peripheral nerve injury. *European Journal of Neuroscience*, 23(3), 617–626. https://doi.org/10.1111/j.1460-9568.2006.04606.x

Chaplan, S. R., Bach, F., Pogrel, J., Chung, J., & Yaksh, T. (1994). Quantitative assessment of tactile allodynia in the rat paw. *Journal of Neuroscience Methods*, 53, 55–63. https://doi.org/10.1016/0165-0270(94)90144-9

Chaudhuri, A. D., Dastgheyb, R. M., Yoo, S.-W., Trout, A., Talbot, C. C., Jr., Hao, H., Witwer, K. W., & Haughey, N. J. (2018). TNFα and IL-1β modify the miRNA cargo of astrocyte shed extracellular vesicles to regulate neurotrophic signaling in neurons. *Cell Death & Disease*, 9(3), 1–18. https://doi.org/10.1038/s41419-018-0369-4

Chen, J., Ren, S., Duscher, D., Kang, Y., Liu, Y., Wang, C., Yuan, M., Guo, G., Xiong, H., Zhan, P., & Wang, Y. (2019). Exosomes from human adipose-derived stem cells promote sciatic nerve regeneration via

optimizing Schwann cell function. *Journal of Cellular Physiology*, *234*(12), 23097–23110. https://doi.org/10.1002/jcp.28873

Chen, Z. L., Yu, M.-W., & Strickland, S. (2007). Peripheral regeneration. *Annual Review of Neuroscience*, *30*, 209–333. https://doi.org/10.1146/annurev.neuro.30.051606.094337

Cheng, L., & Mudge, A. W. (1996). Cultured Schwann cells constitutively express the myelin protein P0. *Neuron*, *16*(2), 309–319. https://doi.org/10.1016/S0896-6273(00)80049-5

Ching, R. C., Wiberg, M., & Kingham, P. J. (2018). Schwann cell-like differentiated adipose stem cells promote neurite outgrowth via secreted exosomes and RNA transfer. *Stem Cell Research & Therapy*, *9*(1), 1–12. https://doi.org/10.1186/s13287-018-1017-8

Colombo, M., Raposo, G., & Théry, C. (2014). Biogenesis, secretion, and intercellular interactions of exosomes and other extracellular vesicles. *Annual Review of Cell and Developmental Biology*, *30*, 255–289. https://doi.org/10.1146/annurev-cellbio-101512-122326

Crookston, K. P., & Gonias, S. L. (1994). The role of cysteine-949 in the binding of transforming growth factor-β1 and transforming growth factor-β2 to α2-macroglobulin. *Biochemical and Biophysical Research Communications*, *200*(3), 1578–1585. https://doi.org/10.1006/bbrc.1994.1631

De Gregorio, C., Contador, D., Campero, M., Ezquer, M., & Ezquer, F. (2018). Characterization of diabetic neuropathy progression in a mouse model of type 2 diabetes mellitus. *Biology Open*, *7*(9), bio036830. https://doi.org/10.1242/bio.036830

Dellarole, A., Morton, P., Brambilla, R., Walters, W., Summers, S., Bernardes, D., Grilli, M., & Bethea, J. R. (2014). Neuropathic pain-induced depressive-like behavior and hippocampal neurogenesis and plasticity are dependent on TNFR1 signaling. *Brain, Behavior, and Immunity*, *41*, 65–81. https://doi.org/10.1016/j.bbi.2014.04.003

Duong, N., Curley, K., Brown, A., Campanelli, A., Do, M. A., Levy, D., Tantry, A., Marriott, G., & Lu, B. (2019). Decoy exosomes as a novel biologic reagent to antagonize inflammation. *International Journal of Nanomedicine*, *14*, 3413–3425. https://doi.org/10.2147/IJN.S196975

Elliott, M. B., Barr, A. E., Clark, B. D., Amin, M., Amin, S., & Barbe, M. F. (2009). High force reaching task induces widespread inflammation, increased spinal cord neurochemicals and neuropathic pain. *Neuroscience*, *158*(2), 922–931. https://doi.org/10.1016/j.neuroscience.2008.10.050

Frühbeis, C., Fröhlich, D., & Krämer-Albers, E.-M. (2012). Emerging roles of exosomes in neuron–glia communication. *Frontiers in Physiology*, *3*, 119. https://doi.org/10.3389/fphys.2012.00119

George, A., Buehl, A., & Sommer, C. (2005). Tumor necrosis factor receptor 1 and 2 proteins are differentially regulated during Wallerian degeneration of mouse sciatic nerve. *Experimental Neurology*, *192*(1), 163–166. https://doi.org/10.1016/j.expneurol.2004.11.002

Gomez-Sanchez, J. A., Carty, L., Iruarrizaga-Lejarreta, M., Palomo-Irigoyen, M., Varela-Rey, M., Griffith, M., Hantke, J., Macias-Camara, N., Azkargorta, M., & Aurrekoetxea, I. (2015). Schwann cell autophagy, myelinophagy, initiates myelin clearance from injured nerves. *Journal of Cell Biology*, *210*(1), 153–168. https://doi.org/10.1083/jcb.201503019

Guma, M., & Firestein, G. S. (2012). Suppl 2: C-Jun N-terminal kinase in inflammation and rheumatic diseases. *The Open Rheumatology Journal*, *6*, 220–231. https://doi.org/10.2174/1874312901206010220

Hawari, F. I., Rouhani, F. N., Cui, X., Yu, Z.-X., Buckley, C., Kaler, M., & Levine, S. J. (2004). Release of full-length 55-kDa TNF receptor 1 in exosome-like vesicles: A mechanism for generation of soluble cytokine receptors. *Proceedings of the National Academy of Sciences*, *101*, 1297–1302. https://doi.org/10.1073/pnas.0307981100

Jia, L., Chopp, M., Wang, L., Lu, X., Szalad, A., & Zhang, Z. G. (2018). Exosomes derived from high-glucose-stimulated Schwann cells promote development of diabetic peripheral neuropathy. *The FASEB Journal*, *32*(12), 6911–6922. https://doi.org/10.1096/fj.201800597R

Jiang, Y., Woronicz, J. D., Liu, W., & Goeddel, D. V. (1999). Prevention of constitutive TNF receptor 1 signaling by silencer of death domains. *Science*, *283*(5401), 543–546. https://doi.org/10.1126/science.283.5401.543

Kalani, A., Tyagi, A., & Tyagi, N. (2014). Exosomes: Mediators of neurodegeneration, neuroprotection and therapeutics. *Molecular Neurobiology*, *49*(1), 590–600. https://doi.org/10.1007/s12035-013-8544-1

Kiguchi, N., Kobayashi, Y., Maeda, T., Saika, F., & Kishioka, S. (2010). CC-chemokine MIP-1α in the spinal cord contributes to nerve injury-induced neuropathic pain. *Neuroscience Letters*, *484*(1), 17–21. https://doi.org/10.1016/j.neulet.2010.07.085

Krämer-Albers, E. M., Bretz, N., Tenzer, S., Winterstein, C., Möbius, W., Berger, H., Nave, K. A., Schild, H., & Trotter, J. (2007). Oligodendrocytes secrete exosomes containing major myelin and stress-protective proteins: Trophic support for axons? *PROTEOMICS–Clinical Applications*, *1*(11), 1446–1461. https://doi.org/10.1002/prca.200700522

Lai, C. P.-K., & Breakefield, X. O. (2012). Role of exosomes/microvesicles in the nervous system and use in emerging therapies. *Frontiers in Physiology*, *3*, 228. https://doi.org/10.3389/fphys.2012.00228

Lee-Kubli, C. A., Ingves, M., Henry, K. W., Shiao, R., Collyer, E., Tuszynski, M. H., & Campana, W. M. (2016). Analysis of the behavioral, cellular and molecular characteristics of pain in severe rodent spinal cord injury. *Experimental Neurology*, *278*, 91–104. https://doi.org/10.3389/fphys.2012.00228

Levine, S. J. (2004). Mechanisms of soluble cytokine receptor generation. *Journal of Immunology*, *173*(9), 5343–5348. https://doi.org/10.4049/jimmunol.173.9.5343

Lopez-Verrilli, M. A. (2012). Transfer of vesicles from schwann cells to axons: A novel mechanism of communication in the peripheral nervous system. *Frontiers in Physiology*, *3*, 205. https://doi.org/10.3389/fphys.2012.00205

Lopez-Verrilli, M. A., Picou, F., & Court, F. A. (2013). Schwann cell-derived exosomes enhance axonal regeneration in the peripheral nervous system. *Glia*, *61*(11), 1795–1806.

Lötvall, J., Hill, A. F., Hochberg, F., Buzás, E. I., Di Vizio, D., Gardiner, C., Gho, Y. S., Kurochkin, I. V., Mathivanan, S., & Quesenberry, P. (2014). Minimal experimental requirements for definition of extracellular vesicles and their functions: A position statement from the International Society for Extracellular Vesicles. *Journal of Extracellular Vesicles*, *3*, 26913. https://doi.org/10.3402/jev.v3.26913

MacEwan, D. J. (2002). TNF receptor subtype signalling: Differences and cellular consequences. *Cellular Signalling*, *14*(6), 477–492. https://doi.org/10.1016/S0898-6568(01)00262-5

Mantuano, E., Henry, K., Yamauchi, T., Hiramatsu, N., Yamauchi, K., Orita, S., Takahashi, K., Lin, J. H., Gonias, S. L., & Campana, W. M. (2011). The unfolded protein response is a major mechanism by which LRP1 regulates Schwann cell survival after injury. *Journal of Neuroscience*, *31*(38), 13376–13385. https://doi.org/10.1523/JNEUROSCI.2850-11.2011

Mathivanan, S., Ji, H., & Simpson, R. J. (2010). Exosomes: Extracellular organelles important in intercellular communication. *Journal of Proteomics*, *73*(10), 1907–1920.

Mazumder, B., Li, X., & Barik, S. (2010). Translation control: A multifaceted regulator of inflammatory response. *Journal of Immunology*, *184*(7), 3311–3319. https://doi.org/10.4049/jimmunol.0903778

Merianda, T. T., Lin, A. C., Lam, J. S., Vuppalanchi, D., Willis, D. E., Karin, N., Holt, C. E., & Twiss, J. L. (2009). A functional equivalent of endoplasmic reticulum and Golgi in axons for secretion of locally synthesized proteins. *Molecular and Cellular Neuroscience*, *40*(2), 128–142. https://doi.org/10.1016/j.mcn.2008.09.008

Myers, R. R., Campana, W. M., & Shubayev, V. I. (2006). The role of neuroinflammation in neuropathic pain: Mechanisms and therapeutic targets. *Drug Discovery Today*, *11*(1–2), 8–20. https://doi.org/10.1016/S1359-6446(05)03637-8

Myers, R. R., Sekiguchi, Y., Kikuchi, S., Scott, B., Medicherla, S., Protter, A., & Campana, W. M. (2003). Inhibition of p38 MAP kinase

activity enhances axonal regeneration. *Experimental Neurology*, *184*(2), 606–614. https://doi.org/10.1016/S0014-4886(03)00297-8

Nelson, B. H. (2004). IL-2, regulatory T cells, and tolerance. *Journal of Immunology*, *172*(7), 3983–3988. https://doi.org/10.4049/jimmunol.172.7.3983

Onda, A., Yabuki, S., & Kikuchi, S. (2003). Effects of neutralizing antibodies to tumor necrosis factor-alpha on nucleus pulposus–induced abnormal nociresponses in rat dorsal horn neurons. *Spine*, *28*(10), 967–972. https://doi.org/10.1097/01.BRS.0000061984.08703.0C

Perrin, F. E., Lacroix, S., Avilés-Trigueros, M., & David, S. (2005). Involvement of monocyte chemoattractant protein-1, macrophage inflammatory protein-1α and interleukin-1β in wallerian degeneration. *Brain*, *128*(4), 854–866. https://doi.org/10.1093/brain/awh407

Plaisance, I., Morandi, C., Murigande, C., & Brink, M. (2008). TNF-α increases protein content in C2C12 and primary myotubes by enhancing protein translation via the TNF-R1, PI3K, and MEK. *American Journal of Physiology - Endocrinology and Metabolism*, *294*(2), E241–E250. https://doi.org/10.1152/ajpendo.00129.2007

Raposo, G., & Stoorvogel, W. (2013). Extracellular vesicles: Exosomes, microvesicles, and friends. *Journal of Cell Biology*, *200*, 373–383. https://doi.org/10.1083/jcb.201211138

Rotshenker, S. (2011). Wallerian degeneration: The innate-immune response to traumatic nerve injury. *Journal of Neuroinflammation*, *8*, 1–14. https://doi.org/10.1186/1742-2094-8-109

Rowlands, D. J., Islam, M. N., Das, S. R., Huertas, A., Quadri, S. K., Horiuchi, K., Inamdar, N., Emin, M. T., Lindert, J., Ten, V. S., Bhattacharya, S., & Bhattacharya, J. (2011). Activation of TNFR1 ectodomain shedding by mitochondrial Ca2+ determines the severity of inflammation in mouse lung microvessels. *Journal of Clinical Investigation*, *121*(5), 1986–1999. https://doi.org/10.1172/JCI43839

Sabio, G., & Davis, R. J. (2014). TNF and MAP kinase signalling pathways. *Seminars in Immunology*, *26*(3), 237–245. https://doi.org/10.1016/j.smim.2014.02.009

Sadri, M., Shu, J., Kachman, S. D., Cui, J., & Zempleni, J. (2020). Milk exosomes and miRNA cross the placenta and promote embryo survival in mice. *Reproduction*, *160*(4), 501–509. https://doi.org/10.1530/REP-19-0521

Sato, S., & Weaver, A. M. (2018). Extracellular vesicles: important collaborators in cancer progression. *Essays in Biochemistry*, *62*(2), 149–163. https://doi.org/10.1042/EBC20170080

Schäfers, M., Brinkhoff, J., Neukirchen, S., Marziniak, M., & Sommer, C. (2001). Combined epineurial therapy with neutralizing antibodies to tumor necrosis factor-alpha and interleukin-1 receptor has an additive effect in reducing neuropathic pain in mice. *Neuroscience Letters*, *310*(2–3), 113–116. https://doi.org/10.1016/S0304-3940(01)02077-8

Schäfers, M., Geis, C., Svensson, C. I., Luo, Z. D., & Sommer, C. (2003). Selective increase of tumour necrosis factor-alpha in injured and spared myelinated primary afferents after chronic constrictive injury of rat sciatic nerve. *European Journal of Neuroscience*, *17*(4), 791–804. https://doi.org/10.1046/j.1460-9568.2003.02504.x

Schäfers, M., & Sorkin, L. (2008). Effect of cytokines on neuronal excitability. *Neuroscience Letters*, *437*(3), 188–193. https://doi.org/10.1016/j.neulet.2008.03.052

Schall, T. J., Lewis, M., Koller, K. J., Lee, A., Rice, G. C., Wong, G. H., Gatanaga, T., Granger, G. A., Lentz, R., & Raab, H. (1990). Molecular cloning and expression of a receptor for human tumor necrosis factor. *Cell*, *61*(2), 361–370. https://doi.org/10.1016/0092-8674(90)90816-W

Schneider-Brachert, W., Tchikov, V., Neumeyer, J., Jakob, M., Winoto-Morbach, S., Held-Feindt, J., Heinrich, M., Merkel, O., Ehrenschwender, M., & Adam, D. (2004). Compartmentalization of TNF receptor 1 signaling: Internalized TNF receptosomes as death signaling vesicles. *Immunity*, *21*(3), 415–428. https://doi.org/10.1016/j.immuni.2004.08.017

Shamash, S., Reichert, F., & Rotshenker, S. (2002). The cytokine network of Wallerian degeneration: Tumor necrosis factor-α, interleukin-1α and interleukin 1β. *Journal of Neuroscience*, *22*(8), 2052–3060. https://doi.org/10.1523/JNEUROSCI.22-08-03052.2002

Shelke, G. V., Lässer, C., Gho, Y. S., & Lötvall, J. (2014). Importance of exosome depletion protocols to eliminate functional and RNA-containing extracellular vesicles from fetal bovine serum. *Journal of Extracellular Vesicles*, *3*(1), 24783. https://doi.org/10.3402/jev.v3.24783

Silveira, A. A. A., Dominical, V. M., Almeida, C. B., Chweih, H., Ferreira, W. A., Jr., Vicente, C. P., Costa, F. T. M., Werneck, C. C., Costa, F. F., & Conran, N. (2018). TNF induces neutrophil adhesion via formin-dependent cytoskeletal reorganization and activation of β-integrin function. *Journal of Leukocyte Biology*, *103*(1), 87–98. https://doi.org/10.1189/jlb.3A0916-388RR

Skoff, A. M., Lisak, R. P., Bealmear, B., & Benjamins, J. A. (1998). TNF-α and TGF-β act synergistically to kill Schwann cells. *Journal of Neuroscience Research*, *53*(6), 747–756. https://doi.org/10.1002/(SICI)1097-4547(19980915)53:6<747::AID-JNR12>3.0.CO;2-V

Sommer, C., Schmidt, C., & George, A. (1998). Hyperalgesia in experimental neuropathy is dependent on the TNF receptor 1. *Experimental Neurology*, *151*(1), 138–142. https://doi.org/10.1006/exnr.1998.6797

Sondell, M., Lundborg, G., & Kanje, M. (1999). Vascular endothelial growth factor has neurotrophic activity and stimulates axonal outgrowth, enhancing cell survival and Schwann cell proliferation in the peripheral nervous system. *Journal of Neuroscience*, *19*(14), 5731–5740. https://doi.org/10.1523/JNEUROSCI.19-14-05731.1999

Sorkin, L. S., & Doom, C. M. (2000). Epineurial application of TNF elicits an acute mechanical hyperalgesia in the awake rat. *Journal of the Peripheral Nervous System*, *5*(2), 96–100. https://doi.org/10.1046/j.1529-8027.2000.00012.x

Subang, M., & Richardson, P. (1999). Tumor necrosis factor-alpha induces monocyte chemoattractant protein-1 mRNA in a Schwann cell line. *Annals of the New York Academy of Sciences*, *883*, 523–525. https://doi.org/10.1111/j.1749-6632.1999.tb08627.x

Tang, P., Hung, M.-C., & Klostergaard, J. (1996). Human pro-tumor necrosis factor is a homotrimer. *Biochemistry*, *35*, 8216–8225. https://doi.org/10.1021/bi952182t

Théry, C., Amigorena, S., Raposo, G., & Clayton, A. (2006). Isolation and characterization of exosomes from cell culture supernatants and biological fluids. *Current Protocols in Cell Biology*, *30*, 3.22. https://doi.org/10.1002/0471143030.cb0322s30

Üçeyler, N., & Sommer, C. (2008). Cytokine regulation in animal models of neuropathic pain and in human diseases. *Neuroscience Letters*, *437*(3), 194–198. https://doi.org/10.1016/j.neulet.2008.03.050

van Niel, G., D'Angelo, G., & Raposo, G. (2018). Shedding light on the cell biology of extracellular vesicles. *Nature Reviews Molecular Cell Biology*, *19*, 213–228.

Vlassov, A. V., Magdaleno, S., Setterquist, R., & Conrad, R. (2012). Exosomes: Current knowledge of their composition, biological functions, and diagnostic and therapeutic potentials. *Biochimica et Biophysica Acta (BBA) - General Subjects*, *1820*(7), 940–948.

Vogel, C., Stallforth, S., & Sommer, C. (2006). Altered pain behavior and regeneration after nerve injury in TNF receptor deficient mice. *Journal of the Peripheral Nervous System*, *11*(4), 294–303. https://doi.org/10.1111/j.1529-8027.2006.00101.x

Wagner, R., & Myers, R. R. (1996). Endoneurial injection of TNF-alpha produces neuropathic pain behaviors. *Neuroreport*, *7*(18), 2897–2901. https://doi.org/10.1097/00001756-199611250-00018

Wagner, R., Myers, R. R., & O'brien, J. S. (1998). Prosaptide prevents hyperalgesia and reduces peripheral TNFR1 expression following TNF-α nerve injection. *Neuroreport*, *9*(12), 2827–2831. https://doi.org/10.1097/00001756-199808240-00026

Weiner, J. A., Fukushima, N., Contos, J. J., Scherer, S. S., & Chun, J. (2001). Regulation of Schwann cell morphology and adhesion by receptor-mediated lysophosphatidic acid signaling. *Journal of Neuroscience*, *21*(18), 7069–7078. https://doi.org/10.1523/JNEUROSCI.21-18-07069.2001

Wollenberg, G. K., Lamarre, J., Rosendal, S., Gonias, S., & Hayes, M. (1991). Binding of tumor necrosis factor alpha to activated forms of human plasma alpha 2 macroglobulin. *The American Journal of Pathology*, *138*(2), 265–272.

Zhang, L., Berta, T., Xu, Z. Z., Liu, T., Park, J. Y., & Ji, R. R. (2011). TNF-alpha contributes to spinal cord synaptic plasticity and inflammatory pain: Distinct role of TNF receptor subtypes 1 and 2. *Pain*, *152*(2), 419–427. https://doi.org/10.1016/j.pain.2010.11.014

Zhang, Z.-J., Cao, D.-L., Zhang, X., Ji, R.-R., & Gao, Y.-J. (2013). Chemokine contribution to neuropathic pain: Respective induction of CXCL1 and CXCR2 in spinal cord astrocytes and neurons. *Pain*, *154*(10), 2185–2197. https://doi.org/10.1016/j.pain.2013.07.002

SUPPORTING INFORMATION

Additional supporting information may be found in the online version of the article at the publisher's website.